A NITSCHE HYBRID MULTISCALE METHOD WITH NON-MATCHING GRIDS

PINGBING MING* AND SIQI SONG[†]

Abstract. We propose a Nitsche method for multiscale partial differential equations, which retrieves the macroscopic information and the local microscopic information at one stroke. We prove the convergence of the method for second order elliptic problem with bounded and measurable coefficients. The rate of convergence may be derived for coefficients with further structures such as periodicity and ergodicity. Extensive numerical results confirm the theoretical predictions.

Key words. Multiscale PDE, hybrid method, Nitsche variational formulation, median analysis

1. Introduction. Consider the elliptic problem with Dirichlet boundary condition

(1.1)
$$\begin{cases} -\operatorname{div}(a^{\varepsilon}(x)\nabla u^{\epsilon}(x)) = f(x), & x \in D \subset \mathbb{R}^d, \\ u^{\epsilon}(x) = 0, & x \in \partial D, \end{cases}$$

where D is a bounded domain and ε is a small parameter that signifies the multiscale nature of the problem. Problem (1.1) may be viewed as a prototypical model of many multiscale problems arising from a variety of contexts, such as the heat conduction and the electromagnetism in composites, or the transport of the porous media. The main quantities of interest for Problem (1.1) are the macroscopical behavior of the solution and the local microscopical information of the solution [14, 8]. Many numerical methods have been developed in the literature to capture either the macroscopical behaviors or the microscopical information of the solution, such as the heterogeneous multiscale methods (HMM) [15], the multiscale finite element methods [27] and among many others.

There are also some methods that aim to retrieve the coarse scale information and the local fine scale information simultaneously. Such methods may be roughly grouped into three classes. The first one is the global-local method, which was originally proposed in [38, 45]. The main idea is to solve the coarse scale problem by a numerical upscaling method firstly, and then solve the local problem around the defects or the places for which the fine scale information is of interest, while the coarse scale information is employed as the constraints. This idea has been incorporated into the HMM framework in [15] and the performance has been thoroughly analyzed in [17] and [7]. The global-local method has been extended to solve an elastodynamical wave equation in [8].

The second method is based on the domain decomposition idea, which has been exploited to solve the multiscale PDEs in [20, 4, 12, 2, 35]. The most relevant is the one in [2]. The authors therein used a discontinuous Galerkin HMM in a region with scale separation, while use a Lagrange finite element method in a region without scale separation. The unknown boundary condition has been supplied by minimizing the difference between the solutions in the overlapped region. The well-posedness and the convergence of this method have been studied in [2] for the periodic media, while the rate of convergence is unknown.

^{*}LSEC, Institute of Computational Mathematics and Scientific/Engineering Computing, AMSS, Chinese Academy of Sciences, No. 55, East Road Zhong-Guan-Cun, Beijing 100190, China and School of Mathematical Sciences, University of Chinese Academy of Sciences, Beijing 100049, China (mpb@lsec.cc.ac.cn,songsq@lsec.cc.ac.cn).

The third method relies on the hybridization idea [28]. One solves the following variational problem: Find $v_h \in X_h$ such that

(1.2)
$$\langle b^{\varepsilon} \nabla v_h, \nabla w \rangle = \langle f, w \rangle$$
 for all $w \in X_h$,

where X_h is any Lagrange finite element space, and we denote the $L^2(D)$ inner product by $\langle \cdot, \cdot \rangle$. Here $b^{\varepsilon}(x) := \rho(x)a^{\varepsilon}(x) + (1 - \rho(x))\mathcal{A}(x)$, where \mathcal{A} is the effective matrix arising from the homogenization problem:

(1.3)
$$\begin{cases} -\operatorname{div}(\mathcal{A}(x)\nabla u_0) = f(x), & x \in D, \\ u_0 = 0, & x \in \partial D. \end{cases}$$

The coefficient b^{ε} is a hybridization of microscopical coefficient and macroscopical coefficient with a transition function ρ . Roughly speaking, the transition function takes one in the defected region and zero otherwise. The authors proved the well-posedness and the convergence of the above hybrid method (1.2) for the bounded and measurable coefficient a^{ε} . The rate of convergence was derived for the periodic media and the quasi-periodic media. Numerical results in [28] show that this hybrid method is comparable with the classical global-local method from both the accuracy and the efficiency, while it is particularly suitable for the scenario that the microscopic coefficient a^{ε} is only available in part of the domain, while outside this region, the coarse scale information is available for the coefficient fields.

The present work is a follow-up of [28], and there are two contributions. Firstly we employ the variational formulation of Nitsche [37] to solve (1.2), which allows for non-matching meshes across the interface. Such numerical interface is caused by the local support of the transition function. The authors in [28] employed a bodyfitted mesh to solve this *interface* problem (1.2). Highly refined mesh has to be used around the defect region to ensure the conformity of the mesh and the resolution of the local defects. From this aspect of view, the non-matching mesh is more flexible in implementation. Indeed, as demonstrated in § 5, fewer global degrees of freedom is required to achieve the desired accuracy compared to the original hybrid method. We note that Nitsche's method is a powerful tool to deal with the interface problem in finite elements and discontinuous Galerkin method; See, e.g., [9, 12, 41]. Another contribution is a general method to construct the transition function, which is an essential ingredient of the hybrid method while seems missing in [28], because only the square defects have been dealt with therein, for which the transition function is a tensor product of a spline function in one dimension. It does not seem easy to find such explicit expression of ρ for defects with irregular shape. Once a general transition function is constructed, it is straightforward to handle the defects with irregular shapes, and numerical results show that the method works well for such irregular defects without occurring extra cost.

To analyze the Nitsche hybrid method, we need a well-defined trace over the element boundary, which demands that $u_0 \in H^{1+s}(D)$ with s > 1/2. For smooth solution, the Nitsche hybrid method may be analyzed by combining the technique in [28] and the standard way for analyzing DG method [6]. Unfortunately, such smoothness assumption on u_0 may not be true for a rough coefficient matrix \mathcal{A} , or a point load function f or a nonconvex domain D. Hence we adapt the median analysis [21] to the present problem. The standard median analysis only works for the matching mesh [21, 22, 33]. To deal with the present case, we construct a new extension operator that measures the difference between the discontinuous finite element space and

the Sobolev space H^1 . The main ingredient of the extension operator is the mesh ratio dependent weights [42, 26] instead of the standard arithmetic mean as in [30]. Using this extension operator, we may prove the error estimate without regularity assumption on u_0 , while the error bounds weakly depend on the mesh ratio. Furthermore, we may remove such dependence by adjusting the the penalized parameter in the Nitsche's variational formulation. Such extension operator is of independent interest and may be useful for analyzing numerical method for interface problem on unfitted mesh [9, 24]. The standard median analysis only works for problems with smooth coefficients or piecewise constant coefficients [30, 21, 22, 33], while we deal with a bounded measurable coefficient a^{ε} which may cause more technical difficulties. We overcome such difficulties by incorporating the oscillations of the coefficients a^{ε} and the load function f into the error bounds.

The rest of the paper is as follows. We introduce the method in § 2. The well-posedness and the error estimates of the proposed method are proved in § 3, this is also the main theoretical results of the present work. We prove the main technical lemmas in § 4. Numerical examples for defects with various shapes are reported in § 5. Some technical results are included in the Appendix.

Throughout this paper, we shall use Sobolev spaces $W^{r,p}(D)$ with norm $\|\cdot\|_{r,p,D}$ and semi-norm $|\cdot|_{r,p,D}$, and we shall drop the subscript p when p=2. We refer to [3] for details. We shall use C as a generic constant independent of ε , the mesh size h, H, and the mesh ratio H/h, which may change from line to line.

2. The Nitsche Hybrid Method. To introduce the method, we firstly fix some notations. Let K_0 be the defected region, and we slightly extend K_0 to K_1 and define $d:=\operatorname{dist}(K_0,K_1)$. Denote $K_2=D\setminus K_1$, and let $|K_i|:=\operatorname{mes}K_i$ with i=1,2 and $\Gamma:=\partial K_1\setminus \partial D$. We refer to Fig. 2_a . Firstly we construct a transition function ρ satisfying

$$\begin{cases} K_1 = \text{supp } \rho, & 0 \le \rho \le 1, \\ \rho(x) \equiv 1 & x \in K_0. \end{cases}$$

To this end, we set $\rho \equiv 1$ in K_0 and $\rho \equiv 0$ outside K_1 . We construct a one layer mesh between K_0 and K_1 . Then, we use a linear Lagrange interpolation over this triangulation to generate the transition function ρ in $K_1 \setminus K_0$, which is a continuous function. The triangulation between K_0 and K_1 for three different kinds of defect is plotted in Fig. 1. This construction ensures that $\rho(x) = 0$ for $x \in \Gamma$. In what

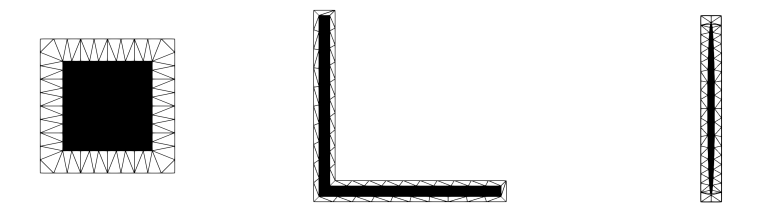
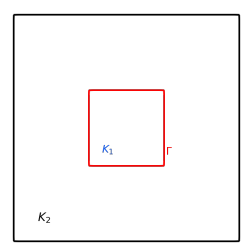


Fig. 1. One layer triangulation of (a) well defect; (b) channel defect; (c) Ellipse defect.

follows, we do not assume any further smoothness on ρ . The effect of the degrees of the smoothness on ρ will be studied in § 5.2.

Now we triangulate K_1 and K_2 with \mathcal{T}_h and \mathcal{T}_H , respectively. Here h and H denote the maximum meshsize of \mathcal{T}_h and \mathcal{T}_H , respectively. Hence, we have a global

triangulation $\mathcal{T}_{h,H} = \mathcal{T}_h \cup \mathcal{T}_H$ over the whole domain though \mathcal{T}_h and \mathcal{T}_H may not be conforming; See Fig. 2 for an illustration of $\mathcal{T}_{h,H}$. We assume that both \mathcal{T}_h and \mathcal{T}_H are shape-regular in the sense of Ciarlet-Raviart [10] with the chunkiness parameter σ .



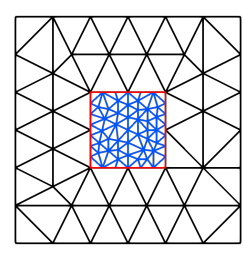


Fig. 2. Left: the region K_1 and K_2 ; Right: The mesh \mathcal{T}_h in K_1 (blue), \mathcal{T}_H in K_2 (black) and the interface Γ (red).

We denote the set of all edges (faces in d=3) of \mathcal{T}_h and \mathcal{T}_H on Γ by \mathcal{E}_h and \mathcal{E}_H , respectively. Moreover, we denote by \mathcal{E}_{\cap} the boundary mesh obtained by intersecting \mathcal{E}_h and \mathcal{E}_H . For convenience, we define

$$\mathcal{T}_h^{\Gamma} := \{ \tau \in \mathcal{T}_h : \overline{\tau} \cap \Gamma \neq \emptyset \} \quad \text{and} \quad \mathcal{T}_H^{\Gamma} := \{ \tau \in \mathcal{T}_H : \overline{\tau} \cap \Gamma \neq \emptyset \},$$

and $\mathcal{T}_{h,H}^{\Gamma} := \mathcal{T}_h^{\Gamma} \cup \mathcal{T}_H^{\Gamma}$. We refer to Fig. 3 for a plot of the mesh around the interface.

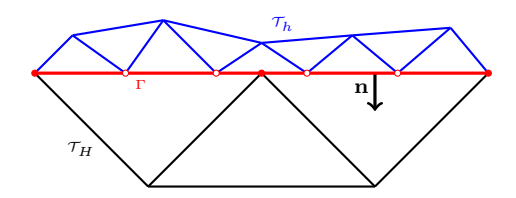


Fig. 3. The collection \mathcal{T}_h^{Γ} (blue) and \mathcal{T}_H^{Γ} (black).

Let X_h and X_H be the Lagrange finite element spaces consisting of piecewise polynomials of degree r-1 over \mathcal{T}_h and \mathcal{T}_H , respectively. Over $\mathcal{T}_{h,H}$, we define

$$(2.1) X_{h,H} := X_h \times X_H \text{ and } X_{h,H}^0 := \{ v \in X_{h,H} | v |_{\partial D} = 0 \}.$$

For each $e \in \mathcal{E}_{\cap}$, there exists $(\tau_1, \tau_2) \in \mathcal{T}_h^{\Gamma} \times \mathcal{T}_H^{\Gamma}$ such that $\bar{\tau}_1 \cap \bar{\tau}_2 = e$. Define $h_e := h_{\tau_1}$ and $H_e := h_{\tau_2}$, and the weighted average and jump for $v = (v_1, v_2) \in X_h \times X_H$ on e are defined by

$$\{\{v\}\}_{\omega} := \omega_1 v_1 + \omega_2 v_2 \text{ and } [\![v]\!] := v_1 - v_2$$

with the weights

$$\omega_1 = \frac{h_e}{h_e + H_e}$$
 and $\omega_2 = \frac{H_e}{h_e + H_e}$.

Similar to the magic DG formula in [6], we have

$$\{\{v\}\}_{\omega} [\![w]\!] - [\![vw]\!] = -[\![v]\!] \{\{w\}\!\}^{\omega},$$

where $\{\{v\}\}^{\omega} := \omega_2 v_1 + \omega_1 v_2$.

The bilinear form is defined for any $v, w \in X_{h,H}$ as

$$\begin{split} B_h^{\varepsilon}(v,w) &:= \sum_{i=1}^2 \int_{K_i} b_h^{\varepsilon} \nabla v \nabla w \, \mathrm{d}x - \sum_{e \in \mathcal{E}_{\cap}} \int_e \left\{ \left\{ b_h^{\varepsilon} \nabla v \cdot \mathbf{n} \right\} \right\}_{\omega} \left[\!\!\left[w\right]\!\!\right] \mathrm{d}s \\ &- \sum_{e \in \mathcal{E}_{\cap}} \int_e \left\{ \left\{ (b_h^{\varepsilon})^T \nabla w \cdot \mathbf{n} \right\} \right\}_{\omega} \left[\!\!\left[v\right]\!\!\right] \mathrm{d}s + \sum_{e \in \mathcal{E}_{\cap}} \int_e \frac{\gamma}{H_e + h_e} \left[\!\!\left[v\right]\!\!\right] \left[\!\!\left[w\right]\!\!\right] \mathrm{d}s, \end{split}$$

where **n** is the unit outward normal vector of Γ from K_1 to K_2 , and γ is the penalized parameter. Here

(2.3)
$$b_h^{\varepsilon}(x) := \rho(x)a^{\varepsilon}(x) + (1 - \rho(x))\mathcal{A}_h(x)$$

with \mathcal{A}_h an approximation of \mathcal{A} . To step further, we assume that a^{ε} belongs to a set $\mathcal{M}(\lambda, \Lambda; D)$ defined by

$$\mathcal{M}(\lambda, \Lambda; D) := \{ a \in [L^{\infty}(D)]^{d \times d} \mid \xi \cdot a(x)\xi \ge \lambda \left| \xi \right|^2, \ \xi \cdot a(x)\xi \ge (1/\Lambda) \left| a(x)\xi \right|^2$$
 for any $\xi \in \mathbb{R}^d$ and $a.e.\ x$ in $D\},$

where $|\cdot|$ denotes the Euclidean norm in \mathbb{R}^d . By the theory of H-convergence [44], we have $\mathcal{A} \in \mathcal{M}(\lambda, \Lambda; D)$. For any reasonable approximation \mathcal{A}_h , we may assume that the hybrid coefficient $b_h^{\varepsilon} \in \mathcal{M}(\lambda', \Lambda'; D)$ for certain positive constants λ' and Λ' . For example, if we use HMM [16, 1, 17, 49] to compute the effective matrix, then $\mathcal{A}_h \in \mathcal{M}(\lambda, \Lambda; D)$. Hence $b_h^{\varepsilon} \in \mathcal{M}(\lambda, \Lambda; D)$. If we use some other numerical upscaling methods, e.g., [18, 32, 19, 29], then $b_h^{\varepsilon} \in \mathcal{M}(\lambda', \Lambda'; D)$ with certain constants λ' and Λ' , which depend on λ and Λ , but not exactly the same. To quantity the approximation error for the effective matrix, we define $e(\mathrm{HMM}) := \max_{x \in \bar{K}_2} \|(\mathcal{A} - \mathcal{A}_h)(x)\|_F$, where $\|\cdot\|_F$ is the Frobenius norm of a matrix.

The approximation problem is defined as: Find $v_h \in X_{h,H}^0$ such that

(2.4)
$$B_h^{\varepsilon}(v_h, w) = \langle f, w \rangle \text{ for all } w \in X_{h,H}^0$$

- 3. Error Estimate for the Nitsche Hybrid Method.
- **3.1. The well-posedness of the method.** For any $v \in X_{h,H}^0$, we define the broken energy norm as

(3.1)
$$|\!|\!|v|\!|\!| := \left(\sum_{i=1}^{2} |v|_{1,K_i}^2 + \sum_{e \in \mathcal{E}_{\cap}} \frac{\gamma}{H_e + h_e} |\!|\!|\!|v|\!|\!|\!|_{0,e}^2\right)^{1/2}.$$

The following lemma gives the continuity and coercivity of the bilinear form B_h^{ε} with respect to the above broken energy norm.

LEMMA 3.1. Assume that b_h^{ε} is in $\mathcal{M}(\lambda', \Lambda'; D)$. Let $\gamma_0 = 8\Lambda'^2 C_{inv}^2 / \min(1, \lambda'^2)$, with C_{inv} in (3.4). If $\gamma \geq \gamma_0$, for all $v, w \in X_{h,H}$, then

$$|B_h^{\varepsilon}(v,w)| \leq 2\Lambda' ||v|| ||w||,$$

(3.3)
$$B_b^{\varepsilon}(v,v) > \min(1/2, \lambda'/2) \|v\|^2$$

where the constant C_{inv} depends only on r and the chunkiness parameter σ such that

$$(3.4) ||v||_{0,e} \le C_{inv} |h_{\tau}|^{-1/2} ||v||_{0,\tau} v \in P_{r-1}(\tau), \ e \subset \partial \tau, \tau \in \mathcal{T}_{h,H}.$$

The existence and uniqueness of the solution of Problem (2.4) follow from the Lax-Milgram theorem provided that $\gamma \geq \gamma_0$. The proof is standard and we refer to [6] for details. The explicit form of C_{inv} may be found in [48], which will be used to determine the lower bound γ_0 of the penalized parameter γ .

3.2. Accuracy for retrieving the macroscopic information. In this part, we estimate the error between the hybrid solution and the homogenized solution. We start with a regularity result for u_0 . By Meyers' regularity result [34], there exists $p_0 > 2$ that depends on D, Λ and λ , such that for all $p \le p_0$,

$$|u_0|_{1,p,D} \le C ||f||_{-1,p,D}$$
,

where C depends on d, D, Λ and λ . Using Hölder's inequality, we obtain

$$(3.5) |u_0|_{1,K_1} \le |K_1|^{1/2-1/p} |u_0|_{1,p,K_1} \le |K_1|^{1/2-1/p} |u_0|_{1,p,D} \le C |K_1|^{1/2-1/p} ||f||_{-1,p,D}.$$

We need an inequality proved in [28, Lemma 3.1].

LEMMA 3.2. For any $v \in H^s(D)$ with $s \in (0,1]$, and for any subset $\Omega \subset D$, there exists C independent of Ω and D such that

(3.6)
$$||v||_{0,\Omega} \le C |\Omega|^{s/d} \eta(\Omega) ||v||_{s,D}$$
,

where

$$\eta(\Omega) = \begin{cases} |\ln |\Omega||^{1/2} & \text{if } d = 2 \text{ and } s = 1, \\ 1 & \text{if } d = 3 \text{ or } s \in (0, 1). \end{cases}$$

The original proof in [28, Lemma 3.1] has not clarified the dependence of the constant C on the domain D, which may be proved by combining the proof in [28, Lemma 3.1] and [13, Remark 6.8].

The following result concerns the accuracy of the method approximating the homogenized solution u_0 when u_0 is smooth.

THEOREM 3.3. Let u_0 and v_h be the solutions of Problem (1.3) and Problem (2.4), respectively. If $u_0 \in H^{1+s}(D)$ with s > 1/2, then there exists C depending on D, λ and Λ such that for any 2 ,

Under the same assumptions, for any 2 with

(3.8)
$$\widetilde{p}_0 = \begin{cases} p_0 & \text{if } d = 2, \\ p_0 \wedge 6 & \text{if } d = 3, \end{cases}$$

we have

$$||u_{0} - v_{h}||_{0,D} \leq C \left(\inf_{\chi \in X_{h,H}^{0}} ||u_{0} - \chi|| + |K_{1}|^{1/2 - 1/p} \right)$$

$$\times \left(\sup_{g \in L^{2}(D)} \frac{1}{||g||_{0,D}} \inf_{\chi \in X_{h,H}^{0}} ||\psi_{g} - \chi|| + |K_{1}|^{1/2 - 1/p} \right)$$

$$+ Ce(\text{HMM}),$$

where $\psi_q \in H_0^1(D)$ is the unique solution of the adjoint variational problem:

(3.10)
$$\langle \mathcal{A} \nabla v, \nabla \psi_q \rangle = \langle g, v \rangle \quad \text{for all} \quad v \in H_0^1(D).$$

To prove Theorem 3.3, we need an auxiliary problem: Find $\widetilde{u} \in X_{h,H}^0$ such that

(3.11)
$$A(\widetilde{u}, v) = \langle f, v \rangle \text{ for all } v \in X_{h, H}^0$$

where the bilinear form A is defined for any $v, w \in X_{h,H}^0$ the same as B_h^{ε} with b_h^{ε} replaced by \mathcal{A} . Proceeding along the same line that leads to Lemma 3.1, we may prove that the bilinear form A is bounded and coercive, which immediately implies the existence and uniqueness of the solution \widetilde{u} . Moreover, we have

LEMMA 3.4. Let $u_0 \in H_0^1(D)$ and $\widetilde{u} \in X_{h,H}^0$ be the solutions of Problem (1.3) and Problem (3.11), respectively. If $u_0 \in H^{1+s}(D)$ with s > 1/2, then

$$|||u_0 - \widetilde{u}||| \le \frac{4\Lambda}{\min(1,\lambda)} \inf_{\chi \in X_{b,H}^0} |||u_0 - \chi|||,$$

and

where $\psi_q \in H_0^1(D)$ is the unique solution of Problem (3.10).

The proof is standard and relies on the Galerkin orthogonality

(3.14)
$$A(u_0 - \widetilde{u}, v) = 0 \quad \text{for any} \quad v \in X_{h,H}^0,$$

which is valid for $u_0 \in H^{1+s}(D)$ with s > 1/2. We omit the details.

Proof of Theorem 3.3 Let $w = \tilde{u} - v_h$, we write

$$\begin{split} B_h^{\varepsilon}(w,w) = & B_h^{\varepsilon}(\widetilde{u},w) - \langle f,w \rangle = B_h^{\varepsilon}(\widetilde{u},w) - A(\widetilde{u},w) \\ = & \sum_{i=1}^2 \int_{K_i} (b_h^{\varepsilon} - \mathcal{A}) \nabla \widetilde{u} \nabla w \, \mathrm{d}x - \sum_{e \in \mathcal{E}_{\cap}} \int_e \left\{ \left\{ (b_h^{\varepsilon} - \mathcal{A}) \nabla \widetilde{u} \cdot \mathbf{n} \right\} \right\}_{\omega} \left[\!\left[\widetilde{u} \right]\!\right] \mathrm{d}s \\ & - \sum_{e \in \mathcal{E}_{\cap}} \int_e \left\{ \left\{ (b_h^{\varepsilon} - \mathcal{A})^T \nabla w \cdot \mathbf{n} \right\} \right\}_{\omega} \left[\!\left[\widetilde{u} \right]\!\right] \mathrm{d}s. \end{split}$$

By
$$b_h^{\varepsilon} - \mathcal{A} = \rho(a^{\varepsilon} - \mathcal{A}) + (1 - \rho)(\mathcal{A}_h - \mathcal{A})$$
, we have, for any $x \in K_1$,
$$\|(b_h^{\varepsilon} - \mathcal{A})(x)\|_F \le \|b_h^{\varepsilon}(x)\|_F + \|\mathcal{A}(x)\|_F \le \Lambda' + \Lambda,$$

and for any $x \in K_2$,

$$\|(b_h^{\varepsilon} - \mathcal{A})(x)\|_F = \|(\mathcal{A}_h - \mathcal{A})(x)\|_F \le e(\text{HMM}).$$

This implies

$$\left| \sum_{i=1}^2 \int_{K_i} (b_h^{\varepsilon} - \mathcal{A}) \nabla \widetilde{u} \nabla w \, \mathrm{d}x \right| \leq (\Lambda + \Lambda') \left| \widetilde{u} \right|_{1,K_1} \left| w \right|_{1,K_1} + e(\mathrm{HMM}) \| \widetilde{u} \| \| w \|.$$

Noting that $\rho = 0$ for $e \in \mathcal{E}_{\cap}$, we obtain for any $x \in e$,

$$\|(b_h^{\varepsilon} - \mathcal{A})(x)\|_F = \|(\mathcal{A}_h - \mathcal{A})(x)\|_F \le e(\text{HMM}).$$

Hence, we obtain

$$\begin{split} & \left| \sum_{e \in \mathcal{E}_{\cap}} \int_{e} \left\{ \left\{ (b_{h}^{\varepsilon} - \mathcal{A}) \nabla \widetilde{u} \cdot \mathbf{n} \right\} \right\}_{\omega} \llbracket w \rrbracket \, \mathrm{d}s \right| \\ & \leq \left(\sum_{e \in \mathcal{E}_{\cap}} \frac{H_{e} + h_{e}}{\gamma} \left\| \left\{ \left\{ (b_{h}^{\varepsilon} - \mathcal{A}) \nabla \widetilde{u} \cdot \mathbf{n} \right\} \right\}_{\omega} \right\|_{0, e}^{2} \right)^{1/2} \left(\sum_{e \in \mathcal{E}_{\cap}} \frac{\gamma}{H_{e} + h_{e}} \left\| \llbracket w \rrbracket \right\|_{0, e}^{2} \right)^{1/2} \\ & \leq \frac{e \left(\mathrm{HMM} \right)}{\gamma_{0}} \left(\sum_{e \in \mathcal{E}_{\cap}} \left(H_{e} + h_{e} \right) \left\| \left\{ \left\{ \nabla \widetilde{u} \right\} \right\}_{\omega} \right\|_{0, e}^{2} \right)^{1/2} \llbracket w \rrbracket. \end{split}$$

Using (3.4), we obtain

$$\sum_{e \in \mathcal{E}_{\cap}} (H_{e} + h_{e}) \| \{ \{ \nabla \widetilde{u} \} \}_{\omega} \|_{0,e}^{2} \leq \sum_{e \in \mathcal{E}_{\cap}} \omega_{1} h_{e} \| \nabla \widetilde{u}_{1} \|_{0,e}^{2} + \sum_{e \in \mathcal{E}_{\cap}} \omega_{2} H_{e} \| \nabla \widetilde{u}_{2} \|_{0,e}^{2} \\
\leq \sum_{e \in \mathcal{E}_{h}} h_{e} \| \nabla \widetilde{u}_{1} \|_{0,e}^{2} + \sum_{E \in \mathcal{E}_{H}} H_{E} \| \nabla \widetilde{u}_{2} \|_{0,E}^{2} \\
\leq C_{\text{inv}} \left(\sum_{\tau \in \mathcal{T}_{h}^{\Gamma}} \| \nabla \widetilde{u}_{1} \|_{0,\tau}^{2} + \sum_{T \in \mathcal{T}_{H}^{\Gamma}} \| \nabla \widetilde{u}_{2} \|_{0,T}^{2} \right).$$

Here, for $e \in \mathcal{E}_h$, h_e denotes the diameter of the element $\tau \in \mathcal{T}_h$ with an edge e and for $E \in \mathcal{E}_H$, H_E denotes the diameter of the element $T \in \mathcal{T}_H$ with an edge E.

A combination of the above two inequalities gives

$$\left| \sum_{e \in \mathcal{E}_{\cap}} \int_{e} \left\{ \left\{ (b_{h}^{\varepsilon} - \mathcal{A}) \nabla \widetilde{u} \cdot \mathbf{n} \right\} \right\}_{\omega} \llbracket w \rrbracket \, \mathrm{d}s \right| \leq \frac{C_{\mathrm{inv}}}{\gamma_{0}} e(\mathrm{HMM}) \lVert \widetilde{u} \rVert \lVert w \rVert.$$

Exchanging the role of \widetilde{u} and w, we obtain

$$\left| \sum_{e \in \mathcal{E}_O} \int_e \left\{ \left\{ (b_h^{\varepsilon} - \mathcal{A})^T \nabla w \cdot \mathbf{n} \right\} \right\}_{\omega} \left[\widetilde{u} \right] \, \mathrm{d}s \right| \leq \frac{C_{\mathrm{inv}}}{\gamma_0} e(\mathrm{HMM}) \left\| \widetilde{u} \right\| \left\| w \right\|.$$

Combining all the above estimates, we obtain

$$(3.15) B_h^{\varepsilon}(w,w) \leq (\Lambda + \Lambda') |\widetilde{u}|_{1,K_1} |w|_{1,K_1} + (1 + 2C_{\mathrm{inv}}/\gamma_0) e(\mathrm{HMM}) |\!|\!|\!|\widetilde{u}|\!|\!|\!|\!|\!|\!||w|\!|\!|\!|.$$

Using the triangle inequality and (3.5), we obtain, for any 2 ,

(3.16)
$$\begin{aligned} |\widetilde{u}|_{1,K_{1}} &\leq |u_{0} - \widetilde{u}|_{1,K_{1}} + |u_{0}|_{1,K_{1}} \\ &\leq ||u_{0} - \widetilde{u}|| + C |K_{1}|^{1/2 - 1/p} ||f||_{-1,p,D}, \end{aligned}$$

and the a-priori estimate $\|\tilde{u}\| \le C \|f\|_{-1,D}$. Combining the above three inequalities, we obtain

$$(3.17) \|\widetilde{u} - v_h\| \le C \left(\|u_0 - \widetilde{u}\| + |K_1|^{1/2 - 1/p} \|f\|_{-1, p, D} + e(\text{HMM}) \|f\|_{-1, D} \right),$$

which together with (3.12) and the triangle inequality conclude the estimate (3.7). We exploit Aubin-Nitsche's dual argument to prove the L^2 error estimate. For any $g \in L^2(D)$, let $\varphi_g \in H^1_0(D)$ satisfying

$$B_h^{\varepsilon}(v, \varphi_q) = \langle g, v \rangle$$
 for all $v \in X_{h,H}$.

Substituting $v = \tilde{u} - v_h$ into the above equation, we obtain

$$\langle g, \widetilde{u} - v_h \rangle = B_h^{\varepsilon}(\widetilde{u} - v_h, \varphi_g) = B_h^{\varepsilon}(\widetilde{u}, \varphi_g) - \langle f, \varphi_g \rangle$$
$$= B_h^{\varepsilon}(\widetilde{u}, \varphi_g) - A(\widetilde{u}, \varphi_g).$$

Proceeding along the same line that leads to (3.15), we obtain

$$|\langle g, \widetilde{u} - v_h \rangle| \le C \left(|\widetilde{u}|_{1,K_1} |\varphi_g|_{1,K_1} + e(\text{HMM}) ||\widetilde{u}|| ||\varphi_g|| \right).$$

Using (3.16), the Meyer's estimate (3.5) to φ_g and the a-priori estimates for \widetilde{u} and φ_g , we obtain, for 2 ,

$$|\langle g, \widetilde{u} - v_h \rangle| \le C |K_1|^{1/2 - 1/p} \left(\|u_0 - \widetilde{u}\| + |K_1|^{1/2 - 1/p} \|f\|_{-1, p, D} \right) \|g\|_{-1, p, D} + Ce(\text{HMM}) \|f\|_{-1, D} \|g\|_{-1, D},$$

Using the Sobolev imbedding $L^2(D) \hookrightarrow W^{-1,p}(D)$ for any $p \ge 1$ if d = 2 and for any $1 \le p \le 6$ if d = 3 [3], we obtain, for any 2 ,

(3.18)
$$\|\widetilde{u} - v_h\|_{0,D} \le C |K_1|^{1/2 - 1/p} \left(\|u_0 - \widetilde{u}\| + |K_1|^{1/2 - 1/p} \|f\|_{-1,p,D} \right) + e(\text{HMM}) \|f\|_{-1,D}.$$

Combining the above inequality with (3.13) and using the triangle inequality, we obtain (3.9).

If we assume an extra regularity condition on the solution u_0 , then

COROLLARY 3.5. If the regularity estimate

(3.19)
$$||u_0||_{1+s,D} \le C ||f||_{0,D}$$
 for $s > 1/2$

is true, then

(3.20)
$$||u_0 - v_h|| \le C(h^s + H^s + |K_1|^{s/d} \eta(K_1) + e(\text{HMM})),$$

$$||u_0 - v_h||_{0,D} \le C\left(h^{2s} + H^{2s} + |K_1|^{2s/d} \eta^2(K_1) + e(\text{HMM})\right).$$

Proof. Let $\Pi_h: H^1(K_1) \mapsto X_h$ and $\Pi_H: H^1(K_2) \mapsto X_H$ be the Scott-Zhang interpolants [39] on K_1 and K_2 , respectively. For any $\tau \in \mathcal{T}_h$,

where ω_{τ} is the local star that contains τ and the elements with nonempty intersection with τ . For any $\tau \in \mathcal{T}_H$,

Define the interpolation $\Pi_{h,H}$ via

$$(\Pi_{h,H}v)|_{K_1} := \Pi_h(v|_{K_1}), \quad (\Pi_{h,H}v)|_{K_2} := \Pi_H(v|_{K_2}).$$

Using (3.21), (3.22) and (3.19), we obtain

$$\sum_{i=1}^{2} |u_0 - \Pi_{h,H} u_0|_{1,K_i}^2 \le C(h^{2s} + H^{2s}) \|f\|_{0,D}^2.$$

Using the trace inequality, (3.21), (3.22) and (3.19), we obtain

$$\begin{split} &\sum_{e \in \mathcal{E}_{\cap}} (H_{e} + h_{e})^{-1} \left\| \left[u_{0} - \Pi_{h,H} u_{0} \right] \right\|_{0,e}^{2} \\ &\leq 2 \sum_{e \in \mathcal{E}_{h}} h_{e}^{-1} \left\| u_{0} - \Pi_{h} u_{0} \right\|_{0,e}^{2} + 2 \sum_{E \in \mathcal{E}_{H}} H_{E}^{-1} \left\| u_{0} - \Pi_{H} u_{0} \right\|_{0,E}^{2} \\ &\leq C \sum_{\tau \in \mathcal{T}_{h}^{\Gamma}} h_{\tau}^{-1} \left(h_{\tau}^{-1} \left\| u_{0} - \Pi_{h} u_{0} \right\|_{0,\tau}^{2} + h_{\tau} \left| u_{0} - \Pi_{h} u_{0} \right|_{1,\tau}^{2} \right) \\ &+ C \sum_{T \in \mathcal{T}_{H}^{\Gamma}} h_{T}^{-1} \left(h_{T}^{-1} \left\| u_{0} - \Pi_{H} u_{0} \right\|_{0,T}^{2} + h_{T} \left| u_{0} - \Pi_{H} u_{0} \right|_{1,T}^{2} \right), \\ &\leq C (h^{2s} + H^{2s}) \left\| f \right\|_{0,D}^{2}. \end{split}$$

Combining the above three estimates, we obtain

$$(3.23) \qquad \inf_{v \in X_{h,H}^0} |||u_0 - \chi||| \le |||u_0 - \Pi_{h,H} u_0||| \le C(h^s + H^s) ||f||_{0,D}.$$

Replacing Meyers' estimate (3.5) with (3.6), we obtain

$$(3.24) |u_0|_{0,K_1} \le C |K_1|^{s/d} \eta(K_1) ||u_0||_{1+s,D} \le C |K_1|^{s/d} \eta(K_1) ||f||_{0,D}.$$

Combining all the above estimates, we obtain (3.20).

If $u_0 \in H^{1+s}(D)$ with $0 < s \le 1/2$, the Galerkin orthogonality (3.14) is invalid and we cannot use Céa's lemma to prove (3.12). To overcome this difficulty, we employ the median analysis in [21]. We firstly need the following extra assumptions on $\mathcal{T}_{h,H}$:

Assumption A: \mathcal{T}_h^{Γ} is quasi-uniform, i.e., there exists a constant ν independent of h_{Γ} such that for any $\tau \in \mathcal{T}_h$, $h_{\tau} \geq \nu h_{\Gamma}$, where $h_{\Gamma} := \max\{h_{\tau} \mid \tau \in \mathcal{T}_h^{\Gamma}\}$.

Assumption B: \mathcal{E}_h is a subgrid of \mathcal{E}_H , i.e., $\mathcal{E}_{\cap} = \mathcal{E}_h$.

According to **Assumption A** and **Assumption B**, we may construct a compatible sub-decomposition $\widetilde{\mathcal{T}}_H^{\Gamma}$ out of \mathcal{T}_H^{Γ} such that $\widetilde{\mathcal{T}}_H^{\Gamma} \cup \mathcal{T}_h^{\Gamma}$ is a conforming mesh, which is quasi-uniform near the interface Γ , while we never need such refined mesh in the implementation; see Fig. 4. Both assumptions have been used in [30] to prove the a-posterior error estimate for the DG method.

We define the oscillation for $f \in L^2(D)$ as

$$\operatorname{osc}(f) := \left[\sum_{\tau \in \mathcal{T}_{h,H}} h_{\tau}^{2} \left(\inf_{\bar{f} \in P_{0}(\tau)} \|f - \bar{f}\|_{0,\tau}^{2} \right) \right]^{1/2},$$

and the oscillation for $A \in [L^{\infty}(D)]^{d \times d}$ as

$$\operatorname{OSC}(\mathcal{A}) := \max_{\tau \in \mathcal{T}_{h,H}} \left(\inf_{\bar{\mathcal{A}} \in [P_0(\tau)]^{d \times d}} \left\| \mathcal{A} - \bar{\mathcal{A}} \right\|_{0,\infty,\tau} \right).$$

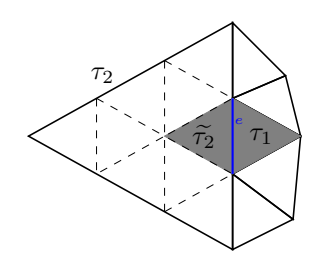


Fig. 4. The split of the element in \mathcal{T}_H^{Γ}

THEOREM 3.6. Let u_0 and v_h be the solutions of Problem (1.3) and Problem (2.4), respectively. If **Assumption A** and **Assumption B** are valid, then there exists C depending on D, λ, Λ and C_{inv} such that for any 2 ,

(3.25)
$$\|u_0 - v_h\| \le C\varrho \left(\inf_{\chi \in X_{h,H}^0} \|u_0 - \chi\| + \operatorname{OSC}(\mathcal{A}) \right) + \operatorname{OSC}(f) \right) + C \left(e(\operatorname{HMM}) + |K_1|^{1/2 - 1/p} \right).$$

Under the same assumptions, for any $2 with <math>\widetilde{p}_0$ defined in (3.8),

$$||u_{0} - v_{h}||_{0,D}$$

$$\leq C \left(\varrho^{2} \left(\inf_{\chi \in X_{h,H}^{0}} |||u_{0} - \chi||| + \operatorname{osc}(f) + \operatorname{osc}(\mathcal{A}) \right) + |K_{1}|^{1/2 - 1/p} \right)$$

$$\times \left(\sup_{g \in L^{2}(D)} \frac{1}{||g||_{0,D}} \inf_{\chi \in X_{h,H}} \left(\sum_{\tau \in \mathcal{T}_{h,H}} h_{\tau}^{-1} ||\psi_{g} - \chi||_{0,\tau} + ||\psi_{g} - \chi||| + \operatorname{osc}(g) \right)$$

$$+ \operatorname{osc}(\mathcal{A}) + |K_{1}|^{1/2 - 1/p} \right) + Ce(\operatorname{HMM}),$$

where $\varrho = (H+h)/(\gamma h_{\Gamma})$ and $\psi_q \in H_0^1(D)$ is the unique solution of Problem (3.10).

The proof of this theorem is a combination of the way leads to Theorem 3.3 and Lemma 3.7 below. We omit the proof.

Lemma 3.7. Under the same assumptions of Theorem 3.6, there exists C depending on D, λ, Λ and C_{inv} such that

$$|||u_0 - \widetilde{u}|| \le C\varrho \left(\inf_{\chi \in X_{h,H}^0} |||u_0 - \chi|| + \operatorname{osc}(f) + \operatorname{osc}(\mathcal{A}) \right),$$

and

$$||u_{0} - \widetilde{u}||_{0,D} \leq C \left(\varrho ||u_{0} - \widetilde{u}|| + \operatorname{osc}(f) + \operatorname{osc}(\mathcal{A}) \right)$$

$$\times \left(\sup_{g \in L^{2}(D)} \frac{1}{||g||_{0,D}} \left(\inf_{\chi \in X_{h,H}} \left(\sum_{\tau \in \mathcal{T}_{h,H}} h_{\tau}^{-1} ||\psi_{g} - \chi||_{0,\tau} + ||\psi_{g} - \chi||_{0} \right) \right) \right)$$

$$+ \operatorname{osc}(g) + \operatorname{osc}(\mathcal{A}),$$

$$(3.28)$$

where $\psi_g \in H_0^1(D)$ is the unique solution of Problem (3.10).

Remark 3.8. By contrast to Lemma 3.4, there is no regularity assumption on u_0 in Lemma 3.7, while it contains extra oscillation terms $\operatorname{osc}(\mathcal{A})$, $\operatorname{osc}(f)$ and $\operatorname{osc}(g)$. Such terms are indispensable by the recent error estimates on Nitsche's mehods [33, 23]. We also note that the right hand side of (3.27) and (3.28) depend on ϱ , which seems unpleasant at the first glance because the error bounds now depend on the mesh ratio, while it may be small or even harmless if we tune the penalized parameter γ . This will be shown in Corollary 3.9 and § 5. It would be very interesting to know whether such dependance can be removed. We shall leave this for further study.

The proof of the above lemma is quite involved and is of independent interest, we postpone it to §4.

If \mathcal{A} and f are smoother, then

COROLLARY 3.9. If $A \in [\mathcal{C}^{0,\alpha}(D)]^{d \times d}$ with $\alpha \in (0,1)$, if we let $\gamma > \max((H+h)/h_{\Gamma}, \gamma_0)$, and if the regularity estimate (3.19) is true for $0 < s \le 1/2$, then

(3.29)
$$||u_0 - v_h|| \le C(h^{\beta} + H^{\beta} + |K_1|^{s/d} \eta(K_1) + e(\text{HMM})),$$

$$||u_0 - v_h||_{0,D} \le C \left(h^{2\beta} + H^{2\beta} + |K_1|^{2s/d} \eta^2(K_1) + e(\text{HMM}) \right),$$

where $\beta = \min(\alpha, s)$.

We omit the proof because the proof is the same with Corollary 3.5.

3.3. Accuracy for retrieving the local microscopic information. We assume that $\operatorname{dist}(K_0,\Gamma)=d\geq \kappa h$ for a sufficiently large $\kappa>0$. For a subset $B\subset D$, we define

$$H^1_{\leq}(B) := \left\{ u \in H^1(D) \mid u|_{D \setminus B} = 0 \right\}, \text{ and } X_{\leq}(B) := \left\{ u \in X_{h,H} \mid u|_{D \setminus B} = 0 \right\}.$$

Let G_1 and G be subsets of K_1 with $G_1 \subset G$ and $\operatorname{dist}(G_1, \partial G \setminus \partial D) = \widetilde{d} > 0$. In order to prove the localized energy error estimate, we state that some properties of the standard Lagrange finite element space X_h hold [11]:

- (1) Local interpolant: There exists a local interpolant Iu such that for any $u \in H^1_{<}(G_1)$, $Iu \in X_{<}(G)$.
- (2) Inverse properties: For each $\chi \in X_{<}(K_1)$, and $\tau \in \mathcal{T}_h$, $1 \leq p \leq q \leq \infty$, and $0 \leq t \leq s \leq r$,

$$\|\chi\|_{s,p,\tau} \le C h_{\tau}^{t-s+n/p-n/q} \|\chi\|_{t,p,\tau} \,.$$

(3) Superapproximation: Let $\omega \in C^{\infty}(K_1) \cap H^1_{<}(G_1)$ with $|\omega|_{j,\infty,K_1} \leq C\widetilde{d}^{-j}$ for integers $0 \leq j \leq r$ for each $\chi \in X_{<}(G) \cap X_h^0$ and for each $\tau \in \mathcal{T}_h$ satisfying $h_{\tau} \leq d$,

THEOREM 3.10. Let u^{ε} and v_h be the solutions of (1.1) and (3.11) respectively. Let $K_0 \subset K_1 \subset D$ be given, and let $dist(K_0, \Gamma) = d$. Let the above properties hold with $\widetilde{d} = d/16$, in addition, let $\max_{\tau \cap \Gamma \neq \emptyset} h_{\tau}/d \leq 1/16$. Then

$$(3.32) |u^{\varepsilon} - v_h|_{1,K_0} \le C \left(\inf_{\chi \in X_h^0} |u^{\varepsilon} - \chi|_{1,K_1} + d^{-1} \|u^{\varepsilon} - v_h\|_{0,K_1} \right),$$

where C depends only on λ' , Λ' , λ , Λ , and D.

Proof. Let a subset $\widetilde{K} \subset K_1$ satisfying $\operatorname{dist}(\widetilde{K},\Gamma) = d_0 > 0$. We have $X_{<}(\widetilde{K}) \subset H^1_{<}(K_1)$. Then for any $v,w \in H^1_{<}(K_1)$, the bilinear form $B_h^{\varepsilon}(v,w)$ degenerates to $\langle b_h^{\varepsilon}v,w\rangle$. Thus, the proof of above theorem is the same with that in [28, Theorem 3.2], and we omit the details for brevity.

Using the triangle inequality, we have

$$|u^{\varepsilon} - v_h|_{1,K_0} \le C \left(\inf_{\chi \in X_{h,H}^0} |u^{\varepsilon} - \chi|_{1,K_1} + d^{-1} \left(\|u_0 - v_h\|_{0,D} + \|u_0 - u^{\varepsilon}\|_{0,D} \right) \right).$$

The first term in the right-hand side of the above inequality concerns how the local events are resolved. Accurate approximation requires a highly refined mesh, which is allowed by Theorem 3.10; using Corollary 3.5 and Corollary 3.9, we may bound $d^{-1} \|u_0 - v_h\|_{0,D}$; the last term converges to zero as ε tends to zero by H-convergence theory [44] for any bounded and measurable a^{ε} . Therefore, the method converges for Problem (1.1) with bounded and measurable coefficient. Moreover, if we assume more structural conditions such as periodicity, almost-periodicity or stochastic ergodicity on a^{ε} , we may expect $\|u^{\varepsilon} - u_0\|_{0,D} \simeq \mathcal{O}(\varepsilon^{\alpha})$ for certain $\alpha > 0$. We refer to [31, 40, 5] for extensive discussions for such L²-estimate.

4. Proof of Lemma 3.4. To prove Lemma 3.4, we employ the median analysis in [21]. We firstly construct an enriching operator $E_h: X_{h,H} \to X_{h,H} \cap H^1(D)$. The construction is similar to that in [30] with certain modifications.

Let $\mathcal{N}(\tau)$ be the set of all nodes of $\tau \in \mathcal{T}_{h,H}$. Define $\mathcal{N}_H := \bigcup_{\tau \in \mathcal{T}_H} \mathcal{N}(\tau)$, $\mathcal{N}_h = \bigcup_{\tau \in \mathcal{T}_h} \mathcal{N}(\tau)$, $\mathcal{N}_\Gamma := \{ p \in \mathcal{N}_h \cup \mathcal{N}_H \mid p \in \Gamma \}$ and $\mathcal{N}_\Gamma^0 := \mathcal{N}_H \cap \mathcal{N}_\Gamma$.

LEMMA 4.1. If Assumption A and Assumption B hold for d=2,3, there exists a linear map $E_h: X_{h,H} \longrightarrow X_{h,H} \cap H^1(D)$ satisfying

(4.1)
$$\sum_{\tau \in T_h^{\Gamma}} h_{\tau}^{2m-2} |v - E_h v|_{m,\tau}^2 \le C \sum_{e \in \mathcal{E}_{\cap}} h_e^{-1} \| [v] \|_{0,e}^2 \quad \text{for all } m \le r - 1,$$

where the constant C is independent of h, H and H/h.

A direct consequence of the above local enriching estimate is the following

COROLLARY 4.2. If **Assumption A** and **Assumption B** are true, then there exists C independent of h, H, γ and the mesh ratio H/h such that

(4.2)
$$\sum_{\tau \in T_{h,H}^{\Gamma}} h_{\tau}^{2m-2} |v - E_h v|_{m,\tau}^2 \le C \varrho ||v||^2, \quad 0 \le m \le r - 1,$$

and

$$|||v - E_h v|||^2 \le C \varrho |||v|||^2,$$

and

(4.5)
$$\sum_{e \in \mathcal{E}_{\cap}} (H_e + h_e) \left| \{ \{ v - E_h v \} \} \right|_{1,e}^2 \le C \varrho ||v||^2.$$

Proof. Using **Assumption A**, we have

$$\sum_{e \in \mathcal{E}_0} h_e^{-1} \left\| [\![v]\!] \right\|_{0,e}^2 \leq \sum_{e \in \mathcal{E}_0} \frac{H_e + h_e}{\gamma h_e} \frac{\gamma}{h_e + H_e} \left\| [\![v]\!] \right\|_{0,e}^2 \leq \varrho |\![v]\!]^2,$$

Therefore, the estimate (4.2) is a direct consequence of (4.1).

Since $v - E_h v \equiv 0$ in $\mathcal{T}_{h,H} \setminus \mathcal{T}_{h,H}^{\Gamma}$, using the above inequality and (4.2) with m = 1, we obtain (4.3).

For any $v = (v_1, v_2) \in X_h \times X_H$, by definition, we obtain

$$\sum_{e \in \mathcal{E}_{\cap}} h_e^{-1} \left\| \left\{ \left\{ v - E_h v \right\} \right\}^{\omega} \right\|_{0,e}^2 \le \sum_{e \in \mathcal{E}_{\cap}} \left(h_e^{-1} \left\| v_1 - E_h v \right\|_{0,e}^2 + h_e^{-1} \omega_1^2 \left\| v_2 - E_h v \right\|_{0,e}^2 \right).$$

Using **Assumption A**, we have, for any $e \in \mathcal{E}_{\cap}$,

$$h_e^{-1}\omega_1^2 \le h_e\omega_1 \le H_e^{-1}$$

Using the trace inequality, there exists C such that

$$\sum_{e \in \mathcal{E}_{\cap}} h_e^{-1} \left\| \left\{ \left\{ v - E_h v \right\} \right\}^{\omega} \right\|_{0,e}^{2} \leq \sum_{e \in \mathcal{E}_h} h_e^{-1} \left| v_1 - E_h v \right|_{1,e}^{2} + \sum_{E \in \mathcal{E}_H} H_E^{-1} \left| v_2 - E_h v \right|_{1,E}^{2}$$

$$\leq C \sum_{\tau \in \mathcal{T}_{h,H}^{\Gamma}} \left(h_{\tau}^{-2} \left\| v - E_h v \right\|_{0,\tau}^{2} + \left| v - E_h v \right|_{1,\tau}^{2} \right),$$

which together with (4.2) implies (4.4).

Proceeding along the same line, we obtain

$$\begin{split} \sum_{e \in \mathcal{E}_{\cap}} (H_{e} + h_{e}) \left| \left\{ \left\{ v - E_{h} v \right\} \right\} \right|_{1,e}^{2} &\leq \sum_{e \in \mathcal{E}_{h}} h_{e} \left| v_{1} - E_{h} v \right|_{1,e}^{2} + \sum_{E \in \mathcal{E}_{H}} H_{E} \left| v_{2} - E_{h} v \right|_{1,E}^{2} \\ &\leq C \sum_{\tau \in \mathcal{T}_{h,H}^{\Gamma}} \left(\left| v - E_{h} v \right|_{1,\tau} + h_{\tau}^{2} \left| v - E_{h} v \right|_{2,\tau} \right), \end{split}$$

which together with (4.2) implies (4.5).

Proof of Lemma 4.1. For any $v \in X_{h,H}$, we define

$$E_hv(p) \coloneqq \begin{cases} v(p) & \text{if} \quad p \in (\mathcal{N}_H \cup \mathcal{N}_h) \setminus \mathcal{N}_\Gamma, \\ \omega_1v_1(p) + \omega_2v_2(p) & \text{if} \quad p \in \mathcal{N}_\Gamma^0, \end{cases}$$

where $v = (v_1, v_2) \in X_h \times X_H$. For each $p \in \mathcal{N}_{\Gamma} \setminus \mathcal{N}_{\Gamma}^0$, there exists $T \in \mathcal{T}_H$ such that p sits on the boundary of T by **Assumption B**. Noting that $E_h v$ is well-defined over T, we may define

$$E_h v(p) := (E_h v)_T(p).$$

The definition of E_h and the uniqueness of the Lagrange interpolation over interface mesh \mathcal{E}_{\cap} ensure that $E_h v$ is continuous across Γ . Therefore, $E_h v \in X_{h,H} \cap H^1(D)$ and $E_h v \equiv v$ in $D \setminus \mathcal{T}_{h,H}^{\Gamma}$.

For $T \in \mathcal{T}_H^{\Gamma}$, we write

$$v - E_h v = \sum_{p \in \mathcal{N}(T) \cap \mathcal{N}_{\Gamma}^0} (v_2 - E_h v)(p) \phi_{T,p}$$
$$= \sum_{p \in \mathcal{N}(T) \cap \mathcal{N}_{\Gamma}^0} \omega_1(v_2 - v_1)(p) \phi_{T,p},$$

where $\phi_{T,p}$ is the Lagrange basis function on T associated with node p. A scaling argument shows that, there exist c_d and C_d independent of h_T such that

$$(4.6) c_d h_T^{d-2m} \le |\phi_{T,p}|_{m,T}^2 \le C_d h_T^{d-2m}.$$

Combining the elements in \mathcal{T}_H^{Γ} and using the standard inverse inequality [10], we obtain

$$\sum_{T \in \mathcal{T}_{H}^{\Gamma}} h_{T}^{2m-2} |v - E_{h}|_{m,T}^{2} \leq C \sum_{e \in \mathcal{E}_{\cap}} \frac{h_{e}^{2}}{(h_{e} + H_{e})^{2}} H_{e}^{d-2} ||\llbracket v \rrbracket ||_{0,\infty,e}^{2} \\
\leq C \sum_{e \in \mathcal{E}_{\cap}} \frac{h_{e}^{2}}{(h_{e} + H_{e})^{2}} H_{e}^{d-2} h_{e}^{-d+1} ||\llbracket v \rrbracket ||_{0,e}^{2} \\
\leq C \sum_{e \in \mathcal{E}_{\cap}} h_{e}^{-1} ||\llbracket v \rrbracket ||_{0,e}^{2},$$
(4.7)

where we have used

$$h_e^{-d+3}H_e^{d-2}/(h_e+H_e)^2 \le (h_e/H_e)^{-d+4}h_e^{-1} \le h_e^{-1}$$
 $d=2,3.$

Next, over each $\tau \in \mathcal{T}_h^{\Gamma}$, we write

$$v - E_h v = \sum_{p \in \mathcal{N}(\tau) \cap \Gamma} (v_1 - E_h v)(p) \phi_{\tau, p}$$
$$= \sum_{p \in \mathcal{N}(\tau) \cap \Gamma} (v_1 - v_2)(p) \phi_{\tau, p} + \sum_{p \in \mathcal{N}(\tau) \cap \Gamma} (v_2 - E_h v)(p) \phi_{\tau, p}$$

By **Assumption B**, there exists $\widetilde{T} \in \mathcal{T}_H$ such that p sits on the boundary of \widetilde{T} , and

$$\begin{split} E_h v(p) - v_2(p) &= \sum_{\widetilde{p} \in \mathcal{N}(\widetilde{T}) \cap \mathcal{N}_{\Gamma}^0} (E_h v - v_2)(\widetilde{p}) \phi_{\widetilde{T}, \widetilde{p}}(p) \\ &= \sum_{\widetilde{p} \in \mathcal{N}(\widetilde{T}) \cap \mathcal{N}_{\Gamma}^0} \omega_1(v_1 - v_2)(\widetilde{p}) \phi_{\widetilde{T}, \widetilde{p}}(p). \end{split}$$

A scaling argument shows that, there exist \widetilde{c}_d and \widetilde{C}_d independent of h_τ such that

$$\widetilde{c}_d h_{\tau}^{d-2m} \le |\phi_{\tau,p}|_{m,\tau}^2 \le \widetilde{C}_d h_{\tau}^{d-2m}$$

By **Assumption A**, the number of the hanging nodes on each $E \in \mathcal{E}_H$ may be bounded by $c(H_E/h_\Gamma)^{d-1}$. Thus, proceeding along the same line that leads to (4.7) and using the above estimate and the inverse inequality, we obtain

$$\sum_{\tau \in \mathcal{T}_{h}^{\Gamma}} h_{\tau}^{2m-2} |v - E_{h}v|_{m,\tau}^{2} \leq C \sum_{e \in \mathcal{E}_{\cap}} h_{e}^{d-2} h_{e}^{-d+1} \| \llbracket v \rrbracket \|_{0,e}^{2} \\
+ C \sum_{e \in \mathcal{E}_{\cap}} (H_{e}/h_{\Gamma})^{d-1} h_{e}^{d-2} h_{e}^{-d+1} \omega_{1}^{2} \| \llbracket v \rrbracket \|_{0,e}^{2} \\
\leq C \sum_{e \in \mathcal{E}_{\cap}} h_{e}^{-1} \| \llbracket v \rrbracket \|_{0,e}^{2} .$$
(4.8)

where we have used

$$(H_e/h_\Gamma)^{d-1}h_e^{-1}\omega_1^2 \le (H_e/h_e)^{d-3}h_e^{-1} \le h_e^{-1} \qquad d=2,3.$$

Combining (4.7) and (4.8), we obtain (4.1).

Next lemma concerns the error estimate of \tilde{u} approximating u_0 , which is a type of *Strang's lemma*, the proof follows from the same line of [21, Lemma 2.1 and § 3.2] and we omit the details.

Lemma 4.3. There exists a constant C such that

$$|||u_0 - \widetilde{u}||| \le C \inf_{\chi \in X_{h,H}^0} \left(|||u_0 - \chi||| + \sup_{\psi \in X_{h,H}^0 \setminus \{0\}} \frac{\langle f, \psi - E_h \psi \rangle - A(\chi, \psi - E_h \psi)}{||\psi||} \right).$$

To estimate the second term in the right hand side of the above inequality, we shall use the following lemma which is similar to the discrete local efficiency estimates in the a-posteriori error analysis [46]. The proof is quite standard and we refer to [47].

LEMMA 4.4. Let $u_0 \in H_0^1(D)$ be the solution of (1.3) and $\chi \in X_{h,H}^0$.

(1) For each $\tau \in \mathcal{T}_{h,H}$, let $\bar{\mathcal{A}} \in [P_0(\tau)]^{d \times d}$, there exists C such that

$$(4.9) h_{\tau}^{2} \| f + \nabla \cdot \bar{\mathcal{A}} \nabla \chi \|_{0,\tau}^{2} \leq C \left(|u_{0} - \chi|_{1,\tau}^{2} + h_{\tau}^{2} \inf_{\bar{f} \in P_{0}(\tau)} \| f - \bar{f} \|_{0,\tau}^{2} + \| \mathcal{A} - \bar{\mathcal{A}} \|_{0,\infty,\tau}^{2} |u_{0}|_{1,\tau}^{2} \right).$$

(2) For each $e \in \mathcal{E}_{\cap}$, there exists $(\tau_1, \widetilde{\tau}_2) \in \mathcal{T}_h^{\Gamma} \times \widetilde{\mathcal{T}}_H^{\Gamma}$ such that $\tau_1 \cap \widetilde{\tau}_2 = e$ and e is a full edge of both τ_1 and $\widetilde{\tau}_2$; See Fig. 4. Let $\overline{\mathcal{A}} \in [P_0(\tau_1) \times P_0(\widetilde{\tau}_2)]^{d \times d}$, we have

(4.10)
$$h_{e} \left\| \left\| \bar{\mathcal{A}} \nabla \chi \cdot \mathbf{n} \right\| \right\|_{0,e}^{2} \leq C \sum_{\tau \in \{\tau_{1}, \tilde{\tau}_{2}\}} \left(\left\| u_{0} - \chi \right\|_{0,\tau}^{2} + h_{\tau}^{2} \inf_{\bar{f} \in P_{0}(\tau)} \left\| f - \bar{f} \right\|_{0,\tau}^{2} + \left\| \mathcal{A} - \bar{\mathcal{A}} \right\|_{0,\infty,\tau}^{2} \left| u_{0} \right|_{1,\tau}^{2} \right).$$

Combining all the above estimates, we are ready to prove Lemma 3.4.

Proof of Lemma 3.4. On each element $\tau \in \mathcal{T}_{h,H}$, let $\bar{\mathcal{A}} \in [P_0(\tau)]^{d \times d}$. We define a bilinear form $\bar{A}(\cdot,\cdot)$ the same as $A(\cdot,\cdot)$ with \mathcal{A} replaced by $\bar{\mathcal{A}}$. For any $\psi \in X_{h,H}^0$, using (2.2), we obtain

$$\langle f, \psi - E_h \psi \rangle - A(\chi, \psi - E_h \psi)$$

$$= \langle f, \psi - E_h \psi \rangle - \bar{A}(\chi, \psi - E_h \psi) + \bar{A}(\chi, \psi - E_h \psi) - A(\chi, \psi - E_h \psi)$$

$$= \sum_{\tau \in \mathcal{T}_{h,H}} \int_{\tau} (f + \nabla \cdot \bar{A} \nabla \chi) (\psi - E_h \psi) \, \mathrm{d}x - \sum_{e \in \mathcal{E}_{\cap}} \int_{e} [\![\bar{A} \nabla \chi \cdot \mathbf{n}]\!] \, \{\![\psi - E_h \psi]\!\}^{\omega} \, \mathrm{d}s$$

$$+ \sum_{e \in \mathcal{E}_{\cap}} \int_{e} \{\![\bar{A}^T \nabla (\psi - E_h \psi) \cdot \mathbf{n}]\!\}_{\omega} [\![u_0 - \chi]\!] \, \mathrm{d}s$$

$$- \sum_{e \in \mathcal{E}_{\cap}} \int_{e} \frac{\gamma}{H_e + h_e} [\![u_0 - \chi]\!] [\![\psi - E_h \psi]\!] \, \mathrm{d}s + (\bar{A}(\chi, \psi - E_h \psi) - A(\chi, \psi - E_h \psi))$$

$$= I_1 + \dots + I_5.$$

Using (4.9) and (4.2) with m = 0, we obtain

$$|I_{1}| \leq \left(\sum_{\tau \in \mathcal{T}_{h,H}} h_{\tau}^{2} \| f + \nabla \cdot \bar{\mathcal{A}} \nabla \chi \|_{0,\tau}^{2}\right)^{1/2} \left(\sum_{\tau \in \mathcal{T}_{h,H}^{\Gamma}} h_{\tau}^{-2} \| \psi - E_{h} \psi \|_{0,\tau}^{2}\right)^{1/2}$$

$$\leq C \varrho \left(\inf_{\chi \in X_{h,H}^{0}} |u_{0} - \chi|_{1,D} + \operatorname{OSC}(f) + \operatorname{OSC}(\mathcal{A})\right) \|\psi\|.$$

Using (4.10) and (4.4), we obtain

$$|I_{2}| \leq \left(\sum_{e \in \mathcal{E}_{\cap}} h_{e} \left\| \left\| \bar{\mathcal{A}} \nabla \chi \cdot \mathbf{n} \right\|_{0,e}^{2} \right)^{1/2} \left(\sum_{e \in \mathcal{E}_{\cap}} h_{e}^{-1} \left\| \left\{ \left\{ \psi - E_{h} \psi \right\} \right\}^{\omega} \right\|_{0,e}^{2} \right)^{1/2}$$

$$\leq C \varrho \left(\inf_{\chi \in X_{h,H}^{0}} |u_{0} - \chi|_{1,D} + \operatorname{osc}(f) + \operatorname{osc}(\mathcal{A}) \right) \|\psi\|.$$

Using (4.5), we obtain

$$|I_{3}| \leq C \left(\sum_{e \in \mathcal{E}_{\cap}} \frac{H_{e} + h_{e}}{\gamma} \left| \left\{ \left\{ \psi - E_{h} \psi \right\} \right\} \right|_{1,e}^{2} \right)^{1/2} \left(\sum_{e \in \mathcal{E}_{\cap}} \frac{\gamma}{H_{e} + h_{e}} \left\| \left[\left[u_{0} - \chi \right] \right] \right\|_{0,e}^{2} \right)^{1/2} \leq C(\varrho/\gamma_{0}) \left\| \left[u_{0} - \chi \right] \right\| \left\| \psi \right\|.$$

Using (4.3), we may bound the last two terms as

$$|I_4| \le C ||u_0 - \chi|| ||\psi||,$$

and

$$|I_5| \leq C \operatorname{osc}(\mathcal{A}) |||\chi|||||\psi - E_h \psi||| \leq C \varrho \operatorname{osc}(\mathcal{A}) \left(|||u_0 - \chi||| + |u_0|_{1,D} \right) |||\psi|||$$

Combining all the above estimates and using Lemma 4.3, we obtain (3.27).

Following the procedure that leads to [21, Theorem 4.4], we shall obtain L^2 estimate (3.28), the proof may be found in the **Appendix A**.

5. Numerical Experiments. In this part, we report two numerical examples with different shapes of defects to demonstrate the accuracy and efficiency of the method. The governing equation is (1.1) with domain $D = (0,1)^2$, the loading function f = 1 and the homogeneous Dirichlet boundary condition is imposed on ∂D . The finite element solvers are carried on FreeFem++ toolbox [25]¹.

The first example is a two-scale example taken from [28].

Example 1: Let

(5.1)
$$a^{\varepsilon}(x) = \frac{(R_1 + R_2 \sin(2\pi x_1)(R_1 + R_2 \cos(2\pi x_2))}{(R_1 + R_2 \sin(2\pi x_1/\varepsilon))(R_1 + R_2 \sin(2\pi x_2/\varepsilon))}I,$$

where I is a two by two identity matrix. The effective matrix is given by

(5.2)
$$\mathcal{A}(x) = \frac{(R_1 + R_2 \sin(2\pi x_1)(R_1 + R_2 \cos(2\pi x_2))}{R_1 \sqrt{R_1^2 - R_2^2}} I.$$

In the simulation we let $R_1 = 2.5$, $R_2 = 1.5$ and $\varepsilon = 0.01$.

We compute u^{ε} and u_0 by directly solving Problem (1.1) and (1.3) with P_1 Lagrange element over a uniform mesh with mesh size around 3.33e-4, respectively. We take these numerical solutions as the reference solutions, which are still denoted by u^{ε} and u_0 , respectively.

The second example is taken from [2] and the coefficient has no clear scale separation inside K_0 .

¹https://freefem.org/

Example 2: For a subset $B \subset D$, we define δ_B as the characteristic function for the set B. The setup for this example is the same with the first one except that the coefficient is replaced by $a^{\varepsilon} = \delta_{K_0}\tilde{a} + (1 - \delta_{K_0})\tilde{a}^{\varepsilon}$, where

$$\tilde{a}(x) = \left(3 + \frac{1}{7} \sum_{j=0}^{4} \sum_{i=1}^{j} \frac{1}{j+1} \cos\left(\left\lfloor 8\left(ix_2 - \frac{x_1}{i+1}\right)\right\rfloor + \lfloor 150ix_1\rfloor + \lfloor 150x_2\rfloor\right)\right) I,$$

and

$$\tilde{a}^{\varepsilon}(x) = (2.1 + \cos(2\pi x_1/\varepsilon)\cos(2\pi x_2/\varepsilon) + \sin(4x_1^2 x_2^2))I.$$

We let $\varepsilon = 0.0063$ in the simulation.

By [28], the effective matrix $\mathcal{A} = \delta_{K_0}\tilde{a} + (1 - \delta_{K_0})\tilde{A}$, where \tilde{A} is the effective matrix associated with \tilde{a}^{ε} . Since there is no analytical formula for \tilde{A} , we use the least-squares based method in [32, 29] to obtain a higher-order approximation to \tilde{A} so that e(HMM) is negligible, which is denoted by \tilde{A}_h . The homogenized solution u_0 is computed by solving Problem (1.3) with $\mathcal{A}_h = \delta_{K_0}\tilde{a} + (1 - \delta_{K_0})\tilde{A}_h$. The hybrid coefficient is

$$b_h^{\varepsilon} = \delta_{K_0} \tilde{a} + (1 - \delta_{K_0}) (\rho \tilde{a}^{\varepsilon} + (1 - \rho) \tilde{A}_h).$$

We use P_1 Lagrange element to compute u^{ε} and u_0 over a refined 3000×3000 mesh as the reference solution.

For both examples, our major interests are the following three quantities:

(5.3)
$$\frac{\|u_0 - v_h\|_{0,K_2}}{\|u_0\|_{0,K_2}}, \quad \frac{|u_0 - v_h|_{1,K_2}}{|u_0|_{1,K_2}} \quad \text{and} \quad \frac{|u^{\varepsilon} - v_h|_{1,K_0}}{|u^{\varepsilon}|_{1,K_0}}.$$

The first two quantities measure the relative accuracy for retrieving the macroscopic information, and the last one quantifies the relative accuracy of the local microscopic information.

5.1. The choice of the penalized factor γ **.** Based on the explicit expressions of the inverse trace inequalities in [48], the lower bound γ_0 in Lemma 3.1 for the penalized factor may be bounded by

(5.4)
$$\gamma_0 \le \begin{cases} \frac{16\sqrt{3}}{9} \frac{r(r+1)\sigma\Lambda'^2}{\min\{1,\lambda'^2\}} & d=2, \\ \frac{32\sqrt{3}}{27} \frac{r(r+2)\sigma\Lambda'^2}{\min\{1,\lambda'^2\}} & d=3. \end{cases}$$

We test **Example 1** and **Example 2** with the well defect (see §5.3.1) for different γ and the results are shown in Fig. 5. We observe that the method works quite well even when γ is less than the threshold value of γ_0 in (5.4), which may be due to that the estimate (5.4) is not sharp. Moreover, the error does not change when γ is bigger than certain threshold value. It is worthwhile to mention that the threshold value does not depend on the mesh ratio H/h. In what follows, we set $\gamma = 50$ in **Example 1** and $\gamma = 20$ in **Example 2**.

5.2. The effect of the smoothness of the transition function. To study the effect of the smoothness of ρ numerically, we consider a square defect K_0 : = $(0.5, 0.5) + (-L, L)^2$ with L = 0.05, and define K_1 : = $(0.5, 0.5) + (-L - \delta, L + \delta)^2$

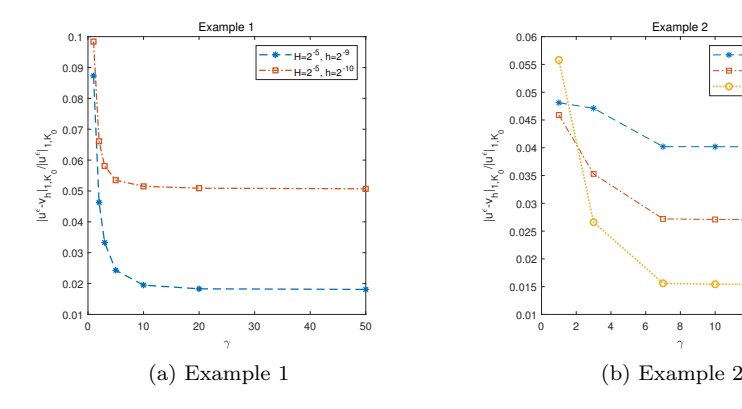


Fig. 5. $|u^{\varepsilon}-v_{h}|_{1,K_{0}}/|u^{\varepsilon}|_{1,K_{0}}$ versus γ in the well defect.

with $\delta = 0.05$. The transition function $\rho = \mu(x_1 - 0.5)\mu(x_2 - 0.5)$ with $\mu : \mathbb{R} \to [0, 1]$ defined by

$$\mu(t) := \begin{cases} \frac{1}{2} \cos \left(\pi(x+L)/\delta \right) + \frac{1}{2}, & \text{if } t \in [-L-\delta, -L), \\ 1 & \text{if } t \in (-L, L), \\ \frac{1}{2} \cos \left(\pi(-x+L)/\delta \right) + \frac{1}{2} & \text{if } t \in (L, L+\delta], \\ 0 & \text{otherwise.} \end{cases}$$

Such ρ is a C¹ function. We test **Example 1** with the above C¹ transition function and the one constructed by a linear interpolant introduced in §2, which is a continuous function. The results are reported in Table 1. It seems that there is no obvious difference between these two choices of ρ . In the following tests, we shall use the linear interpolant transition function.

Table 1 The error of Example 1 with different ρ .

$H = 2^{-5}, h = 2^{-8}$	$ u_0 - v_h _{1,K_2} / u_0 _{1,K_2}$	$ u^{\varepsilon} - v_h _{1,K_0} / u^{\varepsilon} _{1,K_0}$
C^1 transition func.	4.21e-2	1.12e-1
C^0 transition func.	4.21e-2	1.13e-1
$H = 2^{-6}, h = 2^{-9}$	$ u_0 - v_h _{1,K_2} / u_0 _{1,K_2}$	$\left u^{\varepsilon}-v_{h}\right _{1,K_{0}}/\left u^{\varepsilon}\right _{1,K_{0}}$
C^1 transition func.	1.62e-2	4.62e-2
C^0 transition func.	1.62e-2	4.65e-2

- **5.3.** The accuracy of the Nitsche hybrid method. We shall test the examples with the well defect, the channel defect and the ellipse defect to explore the accuracy and the applicability of the Nitsche method.
- **5.3.1. Well defect.** The defect $K_0 = (0.5, 0.5) + (-L, L)^2$ with L = 0.05 is a square, and we define $K_1 := (0.5, 0.5) + (-L \delta, L + \delta)^2$ with $\delta = 0.05$.

We firstly report the results for **Example 1** with a fixed $H = 2^{-5}$ and different h in Table 2. It is shown that that locally refined mesh resolves the local events in this example. We find that the rate of convergence in the energy norm in K_0 is around

the first order, which seems that the term involved h plays the dominant role in the following explicit form of the error estimate (3.32):

$$|u^{\varepsilon} - v_h|_{1,K_0} \le C \left(h + \frac{1}{\delta} (H^2 + L^2 |\ln L| + \varepsilon^{s-1}) \right).$$

The last term comes from the following error estimate proved in [36]:

$$\|u^{\varepsilon} - u_0\|_{0,D} \le C\varepsilon^{s-1} \|u\|_{s,D}$$
 for $s < 3$.

The error between u_0 and v_h in K_2 remains unchanged as h decreased, which shows that the resolution inside the defect has negligible effect on the accuracy for retrieving the macroscopic information.

Table 2

The error of Example 1 in the well defect with $H=2^{-5}$.

h	2^{-7}	2^{-8}	2^{-9}
$ u^{\varepsilon} - v_h _{1,K_0} / u^{\varepsilon} _{1,K_0}$	2.32e-1	1.15e-1	4.60e-2
rate		1.01	1.32
$ u_0 - v_h _{1,K_2} / u_0 _{1,K_2}$	4.60e-2	4.67e-2	4.61e-2

To test the convergence rate between the hybrid solution and the homogenized solution in the subdomain K_2 , we fix the mesh size inside K_1 and vary the mesh size inside K_2 . The result is shown in Table 3. When $H \simeq L$, the second order rate of convergence and the first order rate of convergence are observed for the L^2 error and the energy error, respectively. This is consistent with the following error estimates:

$$||u_0 - v_h||_{0,K_2} \le C(h^2 + H^2 + L^2 |\ln L|), \quad |u_0 - v_h|_{1,K_2} \le C(h + H + L |\ln L|^{1/2}).$$

Nevertheless, the approximation error for the microscopic information remains the same as H varied.

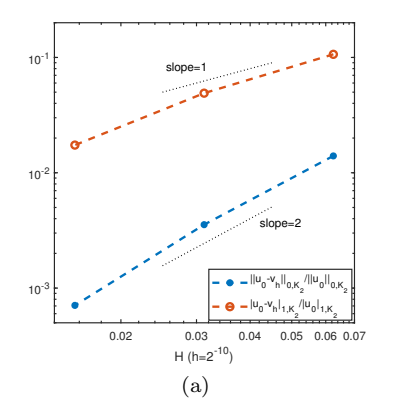
Table 3

The error of Example 1 in the well defect with a fixed $h = 2^{-10}$.

Н	2^{-4}	2^{-5}	2^{-6}
$ u_0 - v_h _{0,K_2} / u_0 _{0,K_2}$	9.87e-3	2.53e-3	6.76e-4
rate		1.96	1.91
$ u_0-v_h _{1,K_2}/ u_0 _{1,K_2}$	1.18e-1	4.61e-2	1.76e-2
rate		1.35	1.39
$ u^{\varepsilon} - v_h _{1,K_0} / u^{\varepsilon} _{1,K_0}$	1.96e-2	1.69e-2	1.66e-2

We turn to **Example 2**. The result in Fig. 6_a shows that the rates of the convergence of the hybrid solution and the homogenized solution in K_2 are optimal with respect to both the energy norm and the L^2 norm. Unfortunately, we do not know any quantity estimate on e(HMM) in this case. Fig. 6_b indicates that the energy error between v_h and u^{ε} inside the defect region K_0 converges at a rate around 0.71, which deteriorates a little bit than the two-scale example. This may be due to the roughness of the coefficients a^{ε} inside K_0 .

5.3.2. Channel defect. We set the defect K_0 as a channel with a corner. Its width is L = 0.05 and K_1 is the set within a distance of $\delta = 0.025$ away from the channel; see Fig. 1_b.



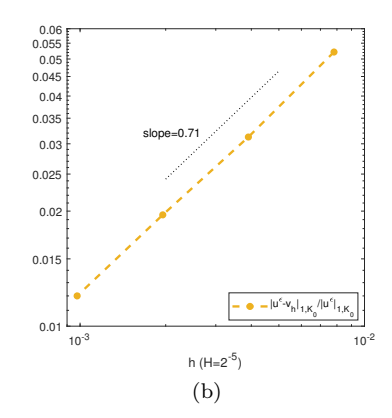


Fig. 6. The error of Example 2 in the well defect.

We firstly test **Example 1** with different H. The result is shown in Table 4. We observe that the first order rate of convergence in the energy norm for the macroscopic information in K_2 , which is consistent with the theoretical result while the convergence rate of L^2 error is less than 2 because the dominant term in the L^2 error is $L |\ln L|$ in this case, i.e.,

$$||u_0 - v_h||_{0,K_2} \le C(h^2 + H^2 + L|\ln L|).$$

 ${\it TABLE 4}$ The error of Example 1 in the channel defect with $h=2^{-9}.$

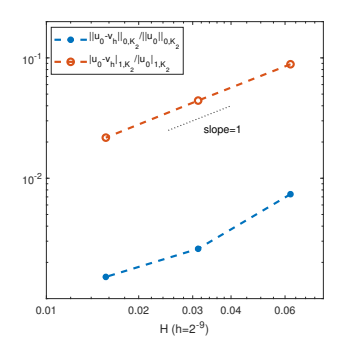
Н	2^{-4}	2^{-5}	2^{-6}
$ u_0 - v_h _{0,K_2} / u_0 _{0,K_2}$	1.12E-2	6.06E-3	4.50E-3
rate		0.89	0.42
$ u_0 - v_h _{1,K_2} / u_0 _{1,K_2}$	9.74E-1	4.86E-2	2.40E-2
rate		1.19	1.00
$ u^{\varepsilon}-v_h _{1,K_0}/ u^{\varepsilon} _{1,K_0}$	7.74e-2	7.73e-2	7.73e-2

Next we fix $H = 2^{-5}$ and vary the mesh size h, and report the result in Table 5. The resolution of defects has more pronounced influence on the accuracy for retrieving the macroscopic accuracy than the well case, especially for the L^2 error.

 $\label{eq:Table 5} {\it Table 5}$ The error of Example 1 in the channel defect with $H=2^{-5}.$

h	2^{-7}	2^{-8}	2^{-9}
$ u^{\varepsilon}-v_h _{1,K_0}/ u^{\varepsilon} _{1,K_0}$	3.69e-1	1.99e-1	7.73e-2
rate		0.90	1.36
$\ u_0 - v_h\ _{0,K_2} / \ u_0\ _{0,K_2}$	2.15e-2	1.04e-2	6.06e-3
$ u_0 - v_h _{1,K_2} / u_0 _{1,K_2}$	5.10e-2	4.90e-2	$4.86\mathrm{e}\text{-}2$

We report the results for **Example 2** in Fig. 7. The method still works with reasonable accuracy. However, the accuracy for approximation the local microscale information is worse than that in **Example 1**, which may be due to the poor regularity of the solution inside K_0 .



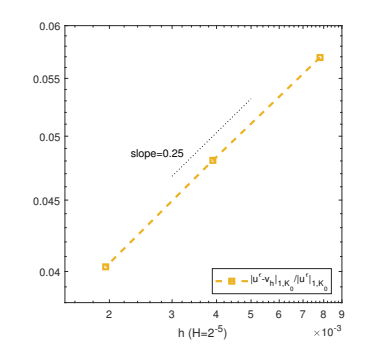


Fig. 7. The error of Example 2 in the channel defect.

5.3.3. Ellipse defects. We choose two slender ellipse defects as K_0 with major axis 0.5 and minor axis 0.02; See Fig. 8. K_1 is a rectangle of size 0.54×0.06 that contains the ellipse; see Fig. 1_c .

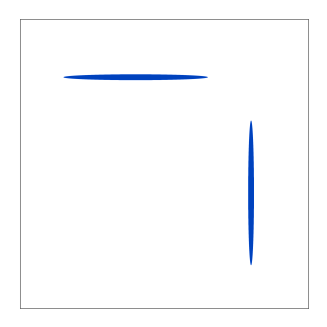


Fig. 8. Ellipse defects

We plot three relative errors from in Fig. 9_a and Fig. 9_b with a fixed ratio H/h. The method works for both examples. If we refine the mesh in both subdomains simultaneously, then the energy error is around the first order, and the L^2 error is around the second order.

5.4. Comparison with the original hybrid method. In the last test, we compare the present method with the hybrid method with a body fitted mesh [28]. Two kinds of mesh are plotted in Fig. 10 for an illustration. Let $K_0 = (0.5, 0.5) + (-L, L)^2$ and $K_1 = (0.5, 0.5) + (-L - \delta, L + \delta)^2$ with L = 0.05 and $\delta = 0.01$. In the non-matching mesh, we choose $h = 10^{-3}$ and $H = 10^{-2}$. In matching mesh,

In the non-matching mesh, we choose $h = 10^{-3}$ and $H = 10^{-2}$. In matching mesh, we construct a body-fitted mesh with the same mesh size. The results for **Example 1** are shown in Table 6. It seems the accuracy of both methods are comparable, while the total degrees of freedom of the Nitsche hybrid method is less than one half of the original hybrid method.

6. Conclusion. We present a hybrid method that captures the macroscopical and microscopical information simultaneously in the framework of the Nitsche's variational formulation. A general method for construction the transition function is

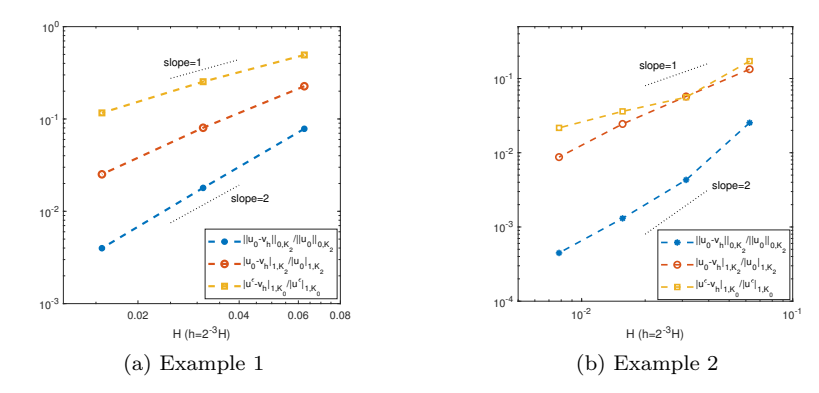


Fig. 9. The relative error for the ellipse defect.

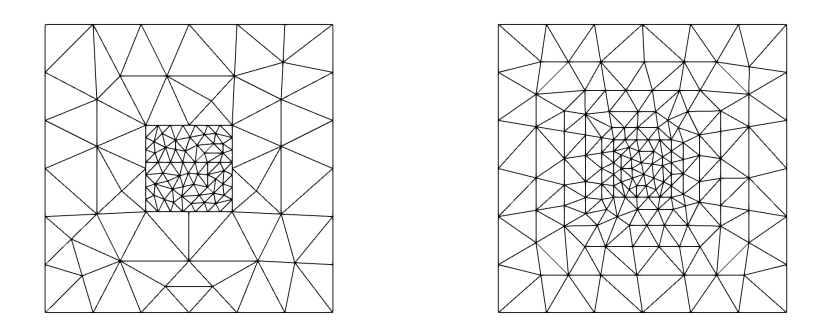


Fig. 10. Left: non-matching mesh; Right: matching mesh.

proposed. This method admits nonmatching mesh and works for defects with irregular shape. Hence the method is more efficient and flexible compared to the original hybrid method [28]. We prove that the method converges for smooth homogenized solution as well as nonsmooth homogenized solution. Rate of convergence has been established for the periodic media and almost-periodic media. A possible extension of the present work is to deal with more realistical problem such as parabolic problems with time varying boundary conditions, which is allowed by the Nitsche's variational formulation [43]. We shall leave this for further pursuit.

Appendix A. Proof of (3.28). For any $\chi \in X_{h,H}^0$, using (3.10) and the enriching operator E_h defined in Lemma 4.1, we obtain

$$\begin{split} \langle g, u_0 - \widetilde{u} \rangle &= \langle g, u_0 - E_h \widetilde{u} \rangle + \langle g, E_h \widetilde{u} - \widetilde{u} \rangle \\ &= \langle \mathcal{A} \nabla (u_0 - E_h \widetilde{u}), \nabla \psi_g \rangle + \langle g, E_h \widetilde{u} - \widetilde{u} \rangle \\ &= \langle f, \psi_g \rangle - \sum_{i=1}^2 \int_{K_i} \mathcal{A} \nabla \widetilde{u} \nabla \psi_g \, \mathrm{d}x + \sum_{i=1}^2 \int_{K_i} \mathcal{A} \nabla (\widetilde{u} - E_h \widetilde{u}) \nabla \psi_g \, \mathrm{d}x \\ &+ \langle g, E_h \widetilde{u} - \widetilde{u} \rangle \,, \end{split}$$

 $\begin{tabular}{ll} Table 6 \\ Comparison between non-matching grid and the matching grid. \end{tabular}$

	Non-matching grid	Matching grid
DOF	28585	60564
$ u^{\varepsilon}-v_h _{1,K_0}/ u^{\varepsilon} _{1,K_0}$	4.60e-2	4.64e-2
$ u_0 - v_h _{1,K_2} / u_0 _{1,K_2}$	9.30e-3	5.66e-3

which may be further expanded as

$$\langle g, u_0 - \widetilde{u} \rangle = \langle f, \chi \rangle - \sum_{i=1}^2 \int_{K_i} \mathcal{A} \nabla \widetilde{u} \nabla \chi \, \mathrm{d}x + \langle f, \psi_g - \chi \rangle - \sum_{i=1}^2 \int_{K_i} \mathcal{A} \nabla \widetilde{u} \nabla (\psi_g - \chi) \, \mathrm{d}x$$
$$+ \langle g, E_h \widetilde{u} - \widetilde{u} \rangle - \sum_{i=1}^2 \int_{K_i} \mathcal{A} \nabla (E_h \widetilde{u} - \widetilde{u}) \nabla \chi \, \mathrm{d}x$$
$$+ \sum_{i=1}^2 \int_{K_i} \mathcal{A} \nabla (\widetilde{u} - E_h \widetilde{u}) \nabla (\psi_g - \chi) \, \mathrm{d}x.$$

Using (3.11), (2.2) and integration by parts, for any piecewise constant matrix $\bar{\mathcal{A}}$ over $\mathcal{T}_{h,H}$, we have

$$\begin{split} & \left\{ \langle g, u_0 - \widetilde{u} \rangle \right. \\ &= \left\{ \left\langle f + \nabla \cdot \bar{\mathcal{A}} \nabla \widetilde{u}, \psi_g - \chi \right\rangle - \sum_{e \in \mathcal{E}_{\cap}} \int_e \left[\left[\bar{\mathcal{A}} \nabla \widetilde{u} \cdot \mathbf{n} \right] \left\{ \left\{ \psi_g - \chi \right\} \right\}^{\omega} \, \mathrm{d}s \right\} \right. \\ & \left. + \left\{ \left\langle g + \nabla \cdot \bar{\mathcal{A}}^T \nabla \chi, E_h \widetilde{u} - \widetilde{u} \right\rangle - \sum_{e \in \mathcal{E}_{\cap}} \int_e \left[\left[\bar{\mathcal{A}}^T \nabla \chi \cdot \mathbf{n} \right] \left\{ \left\{ E_h \widetilde{u} - \widetilde{u} \right\} \right\}^{\omega} \, \mathrm{d}s \right\} \right. \\ & \left. + \left\{ \sum_{i=1}^2 \int_{K_i} \mathcal{A} \nabla (\widetilde{u} - E_h \widetilde{u}) \nabla (\psi_g - \chi) \, \mathrm{d}x + \sum_{e \in \mathcal{E}_{\cap}} \int_e \left. \frac{\gamma}{H_e + h_e} \left[\left[\widetilde{u} \right] \left[\chi \right] \right] \, \mathrm{d}s \right\} \right. \\ & \left. + \left\{ - \sum_{i=1}^2 \int_{K_i} (\mathcal{A} - \bar{\mathcal{A}}) \nabla \widetilde{u} \nabla (\psi_g - \chi) \, \mathrm{d}x - \sum_{e \in \mathcal{E}_{\cap}} \int_e \left\{ \left\{ (\mathcal{A} - \bar{\mathcal{A}}) \nabla \widetilde{u} \right\} \right\}_{\omega} \left[\left[\chi \right] \right] \, \mathrm{d}s \right\} \right. \\ & \left. + \left\{ - \sum_{i=1}^2 \int_{K_i} (\mathcal{A} - \bar{\mathcal{A}}) \nabla (E_h \widetilde{u} - \widetilde{u}) \nabla \chi \, \mathrm{d}x - \sum_{e \in \mathcal{E}_{\cap}} \int_e \left\{ \left\{ (\mathcal{A} - \bar{\mathcal{A}}) \nabla \chi \right\} \right\}_{\omega} \left[\left[\widetilde{u} \right] \right] \, \mathrm{d}s \right\} \right. \\ &= I_1 + \dots + I_5. \end{split}$$

Using Lemma 4.4, we obtain

(A.1)
$$|I_{1}| \leq C \left(\|u_{0} - \widetilde{u}\| + \operatorname{Osc}(f) + \max_{\tau \in \mathcal{T}_{h,H}} \|\mathcal{A} - \bar{\mathcal{A}}\|_{0,\infty,\tau} \|f\|_{-1,D} \right) \times \sum_{\tau \in \mathcal{T}_{h,H}} \left(h_{\tau}^{-1} \|\psi_{g} - \chi\|_{0,\tau} + |\psi_{g} - \chi|_{1,\tau} \right).$$

Using Lemma 4.4 and the enriching estimates (4.2), (4.4), we obtain

$$|I_2| \leq C\varrho \left(\left\| \left\| \psi_g - \chi \right\| + \mathrm{OSC}(g) + \max_{\tau \in \mathcal{T}_{h,H}} \left\| \mathcal{A} - \bar{\mathcal{A}} \right\|_{0,\infty,\tau} \left\| g \right\|_{-1,D} \right) \left\| u_0 - \widetilde{u} \right\|,$$

where we have used the fact $\llbracket u_0 \rrbracket \equiv 0$ on Γ .

Using (4.2) and the fact $\llbracket \psi_q \rrbracket \equiv \llbracket u_0 \rrbracket \equiv 0$ on Γ , we have

$$|I_3| \leq C \varrho \|\widetilde{u} - u_0\| \|\psi_q - \chi\|.$$

Finally,

$$\begin{split} |I_4| &\leq C \max_{\tau \in \mathcal{T}_{h,H}} \left\| \mathcal{A} - \bar{\mathcal{A}} \right\|_{0,\infty,\tau} \left(\sum_{i=1}^2 \left| \widetilde{u} \right|_{1,K_i}^2 \right)^{1/2} \left\| \psi_g - \chi \right\| \\ &\leq C \max_{\tau \in \mathcal{T}_{h,H}} \left\| \mathcal{A} - \bar{\mathcal{A}} \right\|_{0,\infty,\tau} \left(\left\| \left\| u_0 - \widetilde{u} \right\| + \left\| f \right\|_{-1,D} \right) \left\| \psi_g - \chi \right\|, \end{split}$$

and

$$|I_5| \leq C\varrho \max_{\tau \in \mathcal{T}_{h,H}} \left\| \mathcal{A} - \bar{\mathcal{A}} \right\|_{0,\infty,\tau} \left(\left\| \psi_g - \chi \right\| + \left\| g \right\|_{-1,D} \right) \left\| u_0 - \widetilde{u} \right\|.$$

Combining all the above estimates, we obtain (3.28).

Acknowledgments. The authors would like to thank Dr Yufang Huang for the discussion on the topic in the earlier stage of the present work.

REFERENCES

- A. ABDULLE, W. E, B. ENGQUIST, AND E. VANDEN-EIJNDEN, The heterogeneous multiscale method, Acta Numer., 21 (2012), pp. 1–87.
- [2] A. ABDULLE AND O. JECKER, An optimization-based, heterogeneous to homogeneous coupling method, Commun. Math. Sci., 13 (2015), pp. 1639-1648.
- [3] R. A. ADAMS AND J. J. F. FOURNIER, Sobolev Spaces, vol. 140 of Pure and Applied Mathematics (Amsterdam), Elsevier/Academic Press, Amsterdam, second ed., 2003.
- [4] J.-B. APOUNG KAMGA AND O. PIRONNEAU, Numerical zoom for multiscale problems with an application to nuclear waste disposal, J. Comput. Phys., 224 (2007), pp. 403–413.
- [5] S. Armstrong, T. Kuusi, and J.-C. Mourrat, Quantitative Stochastic Homogenization and Large Scale Regularity, Springer Nature Switzerland AG, 2019.
- [6] D. N. ARNOLD, F. BREZZI, B. COCKBURN, AND L. D. MARINI, Unified analysis of discontinuous Galerkin methods for elliptic problems, SIAM J. Numer. Anal., 39 (2001/02), pp. 1749– 1779
- I. Babuška and R. Lipton, L²-global to local projection: an approach to multiscale analysis, Math. Models Methods Appl. Sci., 21 (2011), pp. 2211–2226.
- [8] I. BABUŠKA, M. MOTAMED, AND R. TEMPONE, A stochastic multiscale method for the elastodynamic wave equation arising from fiber composites, Comput. Methods Appl. Mech. Engrg., 276 (2014), pp. 190–211.
- [9] R. BECKER, P. HANSBO, AND R. STENBERG, A finite element method for domain decomposition with non-matching grids, M2AN Math. Model. Numer. Anal., 37 (2003), pp. 209–225.
- [10] P. G. CIARLET, The Finite Element Method for Elliptic Problems, North-Holland Publishing Co., Amsterdam-New York-Oxford, 1978. Studies in Mathematics and its Applications, Vol. 4.
- [11] A. Demlow, J. Guzmán, and A. H. Schatz, Local energy estimates for the finite element method on sharply varying grids, Math. Comp., 80 (2011), pp. 1–9.
- [12] W. DENG AND H. Wu, A combined finite element and multiscale finite element method for the multiscale elliptic problems, Multiscale Model. Simul., 12 (2014), pp. 1424–1457.
- [13] E. DI NEZZA, G. PALATUCCI, AND E. VALDINOCI, Hitchhiker's guide to the fractional Sobolev spaces, Bull. Math. Sci., 136 (2012), pp. 521–573.
- [14] W. E, Principles of Multiscale Modeling, Cambridge University Press, Cambridge, 2011.
- [15] W. E AND B. ENGQUIST, The heterogeneous multiscale methods, Commun. Math. Sci., 1 (2003), pp. 87–132.
- [16] W. E. B. ENGQUIST, X. LI, W. REN, AND E. VANDEN-EIJNDEN, Heterogeneous multiscale methods: a review, Commun. Comput. Phys., 2 (2007), pp. 367–450.
- [17] W. E, P. Ming, and P. Zhang, Analysis of the heterogeneous multiscale method for elliptic homogenization problems, J. Amer. Math. Soc., 18 (2005), pp. 121–156.

- [18] A. GLORIA, Reduction of the resonance error-part 1: approximation of homogenized coefficients, Math. Models Methods Appl. Sci., 21 (2011), pp. 1601–1630.
- [19] A. GLORIA AND M. HABIBI, Reduction in the resonance error in numerical homogenization ii: correctors and extrapolation, Found Comput. Math., 16 (2016), pp. 217–296.
- [20] R. GLOWINSKI, J. HE, J. RAPPAZ, AND J. WAGNER, Approximation of multi-scale elliptic problems using patches of finite elements, C. R. Math. Acad. Sci. Paris, 337 (2003), pp. 679–684.
- [21] T. Gudi, A new error analysis for discontinuous finite element methods for linear elliptic problems, Math. Comp., 79 (2010), pp. 2169–2189.
- [22] T. Gudi, Some nonstandard error analysis of discontinuous Galerkin methods for elliptic problems, Calcolo, 47 (2010), pp. 239–261.
- [23] T. GUSTAFSSON, R. STENBERG, AND J. VIDEMAN, Error analysis of Nitsche's mortar method, Numer. Math., 142 (2019), pp. 973–994.
- [24] P. Hansbo, Nitsche's method for interface problems in computational mechanics, GAMM-Mitt., 28 (2005), pp. 183–206.
- [25] F. HECHT, New development in FreeFem++, J. Numer. Math., 20 (2012), pp. 251-265.
- [26] B. Heinrich and K. Pietsch, Nitsche type mortaring for some elliptic problem with corner singularities, Computing, 68 (2002), pp. 217–238.
- [27] T. Y. Hou and X. H. Wu, A multiscale finite element method for elliptic problems in composite materials and porous media, J. Comput. Phys., 134 (1997), pp. 169–189.
- [28] Y. F. Huang, J. F. Lu, and P. B. Ming, A concurrent global-local numerical method for multiscale PDEs, J. Sci. Comput., 76 (2018), pp. 1188–1215.
- [29] Y. F. HUANG, P. B. MING, AND S. Q. SONG, An efficient online-offline method for elliptic homogenization problems, CSIAM Trans. Appl. Math., 1 (2020), pp. 556-592.
- [30] O. A. KARAKASHIAN AND F. PASCAL, A posteriori error estimates for a discontinuous Galerkin approximation of second-order elliptic problems, SIAM J. Numer. Anal., 41 (2003), pp. 2374–2399.
- [31] C. Kenig, F. H. Lin, and Z. W. Shen, Convergence rates in L² for elliptic homogenization problems, Arch. Rational Mech. Anal., 203 (2012), pp. 1009–1036.
- [32] R. LI, P. B. MING, AND F. Y. TANG, An efficient high order heterogeneous multiscale method for elliptic problems, Multiscale Model. Simul., 10 (2012), pp. 259–283.
- [33] N. LÜTHEN, M. JUNTUNEN, AND R. STENBERG, An improved a priori error analysis of Nitsche's method for Robin boundary conditions, Numer. Math., 138 (2018), pp. 1011–1026.
- [34] N. G. MEYERS, An L^p-estimate for the gradient of solutions of second order elliptic divergence equations, Ann. Scuola Norm. Sup. Pisa Cl. Sci. (3), 17 (1963), pp. 189–206.
- [35] P. B. MING AND X. M. Xu, A multiscale finite element method for oscillating Neumann problem on rough domain, Multiscale Model. Simu., 14 (2016), pp. 1276–1300.
- [36] S. Moskow and M. Vogelius, First order corrections to the homogenized eigenvalues of a periodic composite medium. a convergence proof, Proc. Roy. Soc. Edinburgh, 127 (1997), pp. 1263–1295.
- [37] J. A. NITSCHE, Über ein Variationsprinzip zur Lösung von Dirichlet-Problemen bei Verwendung von Teilräumen, die keinen Randbedingungen unterworfen sind, Abh. Math. Sem. Univ. Hamburg, 36 (1971), pp. 9–15.
- [38] J. T. Oden and K. S. Vemaganti, Estimation of local modeling error and goal-oriented adaptive modeling of heterogeneous materials. I. Error estimates and adaptive algorithms, J. Comput. Phys., 164 (2000), pp. 22–47.
- [39] L. R. SCOTT AND S. Y. ZHANG, Finite element interpolation of nonsmooth functions satisfying boundary conditions, Math. Comp., 54 (1990), pp. 483–493.
- [40] Z. W. Shen, Convergence rates and Hölder estimates in almost-periodic homogenization of elliptic systems, Analysis and PDE, 8 (2015), pp. 1565–1601.
- [41] F. Song, W. B. Deng, and H. J. Wu, A combined finite element and oversampling multiscale Petrov-Galerkin method for the multiscale elliptic problems with singularities, J. Comput. Phys., 305 (2016), pp. 722–743.
- [42] R. STENBERG, Mortaring by a method of J. A. Nitsche, in Computational Mechanics (Buenos Aires, 1998), Centro Internac. Métodos Numér. Ing., Barcelona, 1998, pp. CD–ROM file.
- [43] A. Tagliabue, L. Dedé, and A. Quarteroni, Nitsche'e method for parabolic partial differential equations with mixed time varying boundary conditions.
- [44] L. TARTAR, The General Theory of Homogenization: A Personalized Introduction, vol. 7 of Lecture Notes of the Unione Matematica Italiana, Springer-Verlag, Berlin; UMI, Bologna, 2009.
- [45] K. S. Vemaganti and J. T. Oden, Estimation of local modeling error and goal-oriented adaptive modeling of heterogeneous materials. II. A computational environment for adaptive modeling of heterogeneous elastic solids, Comput. Methods Appl. Mech. Engrg., 190 (2001),

- pp. 6089–6124.
- [46] R. Verfürth, A posteriori error estimation and adaptive mesh-refinement techniques, in Proceedings of the Fifth International Congress on Computational and Applied Mathematics (Leuven, 1992), vol. 50, 1994, pp. 67–83.
- [47] R. Verfürth, A Posteriori Error Estimation Techniques for Finite Element Methods, Numerical Mathematics and Scientific Computation, Oxford University Press, Oxford, 2013.
- [48] T. WARBURTON AND J. S. HESTHAVEN, On the constants in hp-finite element trace inverse inequalities, Comput. Methods Appl. Mech. Engrg., 192 (2003), pp. 2765–2773.
- [49] X. Y. Yue and W. E, The local microscale problem in the multiscale modeling of strongly heterogeneous media: effects of boundary conditions and cell size, J. Comput. Phys., 222 (2007), pp. 556-572.